1000-0569/2019/035(01)-0215-32 *Acta Petrologica Sinica* 岩石学报 doi: 10.18654/1000-0569/2019.01.17

稀有气体同位素地球化学在矿床学研究中的应用进展*

武丽艳

WU LiYan

中国科学院地球化学研究所,矿床地球化学国家重点实验室,贵阳 550081

State Key Laboratory of Ore Deposit Geochemistry, Institute of Geochemistry, Chinese Academy of Sciences, Guiyang 550081, *China*

2018-07-29 **收稿**, 2018-10-19 **改回**.

Wu LY. 2019. Advances of noble gas isotope geochemistry application in the study of ore deposits. *Acta Petrologica Sinica*, 35(1):215 – 232, doi:10.18654/1000-0569/2019.01.17

Abstract Due to the chemical inertness and the distinct isotopic composition in different reservoirs, noble gas isotopes are playing important role in tracing ore-forming fluid origin, evolution and the process of crust-mantle interaction. Besides, as ^{4}He and ^{40}Ar has the effect of time accumulation, they are often used for dating. In this paper, we briefly reviews the modification of noble gas isotopes in fluid inclusions by post-entrapment processes and matters needing attention in the selection of samples and analytical methods, the progress of the noble gas in tracing ore-forming fluid origin, ^{40}K-^{40}Ar and ^{40}Ar-^{39}Ar dating, as well as (U-Th)/He dating. We conclude that noble gas isotopes in fluid inclusions can be modified by addition of cosmogenic ^{3}He, in situ produced ^{4}He and He loss. Analysis methods should be selected according to the purpose. Noble gas isotopes can be used to trace the origin and evolution of ore-forming fluid, and crust-mantle interaction of different types of deposits. In addition, noble gas isotopes combined with halogens can be used to indicate the origin and evolution of ore-forming fluids and salinity, as well as the mechanism of mineral precipitation. ^{3}He/heat ratio can be used to trace the heat source and its transport mode of fluid. The $^{40}Ar/^{39}Ar$ progressive crushing and stepwise heating techniques can be used to directly determine the mineralization ages of hydrothermal sulfide deposits. ^{40}K-^{40}Ar and/or ^{40}Ar-^{39}Ar dating of supergene K-bearing minerals and (U-Th)/He dating of iron oxides can be used to determine the chronology of deposits and related oxidation zone. Based on the different close temperature of minerals, ^{40}K-^{40}Ar and/or ^{40}Ar-^{39}Ar dating of K-bearing minerals and (U-Th)/He dating of zircon, apatite and iron oxides provide a large amount of meaningful information for history of uplift and exhumation after deposit formation, and paleoclimate evolution.

Key words Tracing ore-forming fluid; Noble gas and halogen; ^{3}He/heat; ^{40}Ar-^{39}Ar dating; (U-Th)/He dating

摘 要 稀有气体因其化学惰性以及在不同来源地质体中的同位素组成差异很大,在研究成矿流体来源、演化和壳-幔相互作用过程中具有非常重要的意义。另外,由于^{4}He、^{40}Ar是放射成因子体同位素,具有年代积累效应,因此,它们常被用于同位素测年。本文简要回顾了流体包裹体中稀有气体同位素的后生影响和样品、分析方法选择注意事项,以及近年来稀有气体同位素在成矿流体示踪,^{40}K-^{40}Ar、^{40}Ar-^{39}Ar定年及(U-Th)/He定年方面的研究进展。已有研究证实流体包裹体中的稀有气体可能受后期扩散丢失、后生叠加和同位素分馏的影响,要根据目的选择不同的分析方法;稀有气体同位素可以示踪不同类型矿床的流体来源、演化及壳-幔相互作用、稀有气体同位素与卤素联合运用可以用来指示流体和盐度来源、演化过程以及矿物沉淀机制等,^{3}He/热的研究可以追溯流体的热源及其运移方式;流体包裹体^{40}Ar-^{39}Ar可以用于矿床直接定年,表生含钾矿物的^{40}K-^{40}Ar、^{40}Ar-^{39}Ar定年以及锆石、磷灰石和铁氧化物(U-Th)/He定年可为矿床及氧化带的形成时间、矿床形成后的抬升、剥露历史、古气候演化等重大地质问题讨论提供大量有意义的信息。

关键词 稀有气体;流体示踪;^{3}He/热;^{40}Ar-^{39}Ar定年;(U-Th)/He定年

中图法分类号 P597

---

* 本文受中国科学院战略性先导专项(B类)(XDB18000000)、国家重点研发项目(2016YFC0600207)和国家自然科学基金项目(41773048)联合资助.

第一作者简介:武丽艳,女,1981年生,副研究员,矿物学、岩石学、矿床学专业,E-mail: wuliyan@mail.gyig.ac.cn

稀有气体(主要包括 He、Ne、Ar、Kr 和 Xe)因其在地球中含量稀少和化学性质不活泼,在太阳系起源、行星演化、地球形成、地幔演化及其动力学、矿床成因、流体来源及演化等方面被广泛应用。目前,稀有气体同位素在矿床学中的应用主要集中在成矿流体的示踪和年代学两个方面。由于人们对大气、地壳、上、下地幔等不同来源物质的 He、Ar 同位素组成有了较为清晰的认识,因此,在矿床学研究中,作为灵敏示踪剂的稀有气体同位素大多用于判别成矿流体的来源,特别是幔源物质的贡献大小及壳幔相互作用与成矿的关系(Hu *et al.*, 1998a, c, 2012; 胡瑞忠等, 1999; Burnard *et al.*, 1999; Burnard and Polya, 2004; Kendrick *et al.*, 2001a; Manning and Hofstra, 2017; Xie *et al.*, 2016; Desanois *et al.*, 2018; Wu *et al.*, 2018a),用于揭示矿床在成矿各阶段(期)中的物质和流体源区差异,以及追踪和揭示成矿流体的演化、反演成矿过程(Irwin and Roedder, 1995; Kendrick *et al.*, 2011a, b; Richard *et al.*, 2014)。另外,由于 ^{4}He、^{40}Ar 具有年代积累效应,因此,它们常被用于同位素测年。尤其是近年来人们对矿床形成后的改造-保存过程的关注,低温热年代学比如裂变径迹、(U-Th)/He、含钾矿物 K-Ar、^{40}Ar-^{39}Ar 等定年方法被用于厘定表生矿物年龄、探讨矿床的隆升、剥蚀速率和剥蚀量等,揭示矿床的保存条件及预测隐伏矿床(Vasconcelos *et al.*, 1992, 1994a; Vasconcelos and Conroy, 2003; Reiners *et al.*, 2003; Harris *et al.*, 2008; 许英霞等, 2008; 何为等, 2009; Chen and Li, 2014; Bonnet *et al.*, 2016; Yang *et al.*, 2016; 喻顺等, 2016; Ershova *et al.*, 2018)。为进一步推动稀有气体同位素研究工作在我国的发展,本文回顾了近年来稀有气体同位素在矿床成矿流体示踪和年代学研究方面取得的重要进展,供感兴趣的专家、学者参考和借鉴。

1 样品选择及注意事项

保存在矿物中的原生流体包裹体的成分近似于矿床形成时的成矿流体的组成,因而,通过对矿物原生包裹体稀有气体同位素组成的研究,可以进行流体来源的示踪。但是,从矿物形成到被开采出来,样品经历了一系列的地质作用。因此,样品流体包裹体中的稀有气体除了来自当时的成矿流体外,还可能受后期扩散丢失、后生叠加和同位素分馏的影响(Stuart *et al.*, 1994a)。

1.1 扩散丢失的影响

稀有气体在矿物中扩散丢失的量与寄主矿物扩散系数的大小成正比。研究表明,硫酸盐和硫化物对稀有气体具有较好的保存能力(Trull *et al.*, 1991; Jean-Baptiste and Fouquet, 1996)。尤其是硫化物中的黄铁矿具有很低的 He 扩散系数(Jean-Baptiste and Fouquet, 1996),即使是最容易扩散的 He,在封闭后的 100Ma 时间内,也不会发生明显的扩散丢失(Stuart *et al.*, 1994a),而且即使有稀有气体的扩散,其扩散所产生的同位素分馏效应极小且基本可以忽略不计(胡瑞忠等, 1999; Ballentine and Burnard, 2002; Hu *et al.*, 2004)。而石英等透明矿物虽然对于 Ar 具有很好的保存能力(Trull *et al.*, 1991; 胡瑞忠等, 1999),但流体包裹体中的 He 则很容易发生扩散丢失(Turner *et al.*, 1993; Stuart *et al.*, 1994a; 胡瑞忠等, 1999),如图 1 所示,与硫化物相比,石英中 He、Ar 组成具有明显的 He 丢失趋势,但 $^{3}He/^{4}He$ 比值基本没受影响(胡瑞忠等, 1999)。因此,石英等透明矿物中流体包裹体的浓度不能代表其捕获时的浓度。但是,He 扩散所产生的同位素分馏效应极小且基本可以忽略不计,对应用 He 同位素比值讨论成矿流体来源和演化不会产生根本影响。另外,Kendrick *et al.* (2005)的研究发现硫酸钡和方铅矿有时具有漏 He 特征。因此,在做流体包裹体中稀有气体同位素分析时,应避免选择对稀有气体保存能力不好的矿物。

1.2 原位放射成因和宇宙成因 He 的影响

^{238}U、^{235}U 和 ^{232}Th 的衰变会产生 ^{4}He,K 的衰变可产生

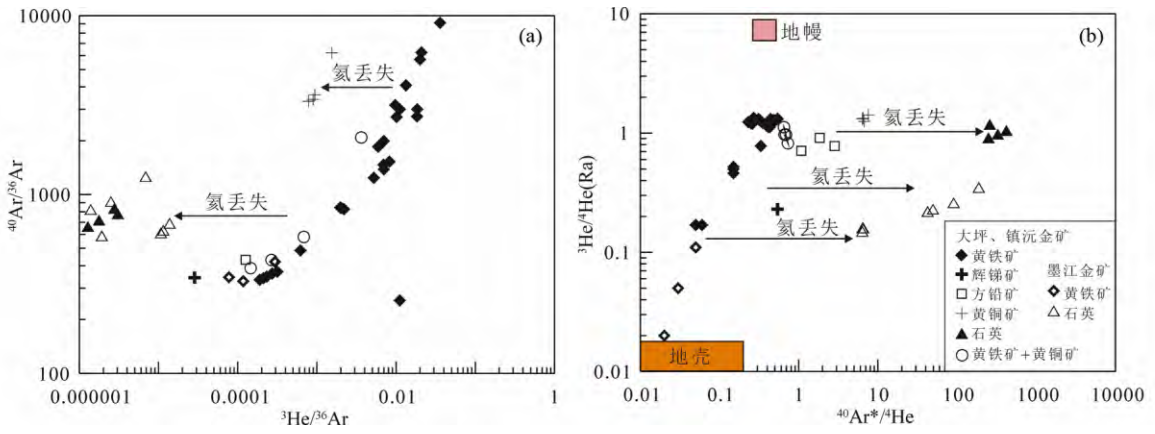

图 1 He 在石英流体包裹体中的扩散丢失(据胡瑞忠等, 1999)

Fig. 1 Diffusion loss of He in quartz fluid inclusion (after Hu *et al.*, 1999)

^{40}Ar。因此,寄主矿物或流体包裹体中的 U、Th、K 等放射性元素的存在会对包裹体中稀有气体同位素的组成产生影响。但一般情况下,除了钾和含钾矿物,铀和含铀矿物外,其他矿物流体包裹体中 U、Th、K 含量很低(Th 在热液中几乎是不溶的),且由于 α 粒子停止距离的影响,放射成因 ^{4}He 对于直径小于 20μm 的流体包裹体中 ^{4}He 也不会产生影响(Stuart *et al.*, 1994a);即便如此,放射成因 ^{4}He 和 ^{40}Ar 的影响也可根据成矿年龄、流体包裹体中或全岩或围岩的 U、Th、K 含量,做定量的模拟计算(Craig and Lupton, 1976; Ballentine and Burnard, 2002),以评估捕获后放射性成因 ^{4}He 和 ^{40}Ar 累积的影响。宇宙射线产生 ^{3}He 主要受反应 $^{6}Li(n, \alpha)^{3}H(\beta)^{3}He$ 和重核裂变的控制(Kurz, 1986),但一般只在地表范围(约 1.5m)影响比较大(Kurz, 1986; Stuart *et al.*, 1995)。因此,采自地表 1.5m 以下的样品中宇宙成因 He 的影响可忽略不计。

1.3 同位素分馏及其他因素的影响

研究表明,稀有气体同位素在包裹体捕获及提取过程中都不会产生明显的同位素分馏(Podosek *et al.*, 1981; Turner and Wang, 1992; Jean-Baptiste and Fouquet, 1996)。矿物形成后,后期改造形成的次生包裹体中的稀有气体丰度和同位素组成也会影响原始成矿流体的稀有气体同位素组成。研究表明,用逐步压碎技术首先释放的是次生包裹体,最后释放原生包裹体,中间为两者混合,但当样品粉末粒度小于 0.5μm 时,继续破碎可能会释放出矿物晶格内的气体(Qiu and Wijbrans, 2008; Jiang *et al.*, 2012; Bai *et al.*, 2013, 2018)。因此,在进行测试时,应选择晶形完好、未受后期改造的矿物。另外,由于大气中 He 的含量极低,因此,不足以对地壳流体中氦的丰度和同位素组成产生明显影响(Stuart *et al.*, 1994b)。虽然严格的分析程序可以最大限度地减少大气中 Ar 在样品和破碎装置表面的吸附,但大气 Ar 的影响不能完全清除。

1.4 分析方法的选择

固体样品中稀有气体的提取方式主要有三种: 压碎法、加热熔融法和激光熔蚀法。压碎法是矿床学研究中获取矿物包裹体中稀有气体的主要方式,一般不会释放矿物晶格中的气体,可以将后期放射性成因稀有气体和大气的影响降至最低(Stuart *et al.*, 1995),且分阶段压碎可能会获取不同包裹体群组的成分信息(Qiu and Wijbrans, 2008; Jiang *et al.*, 2012; Bai *et al.*, 2013, 2018)。而加热熔融法不仅释放包裹体和岩矿石裂隙中的气体,而且晶格中的气体也会被释放出来。分阶段加热熔融可以通过设定温度来获取前期捕获和后期放射性成因的气体(Stuart *et al.*, 1995; Pettke *et al.*, 1997),而要获得流体包裹体中卤素的成分又通常需要对矿物采用阶段加热法(Kendrick *et al.*, 2001b);但是,对于硫化物和硫酸盐通常不用加热法以免加热过程产生的 SO_2 污染系统。激光熔蚀法可以有针对性地精确释放所选微区的气体。叶先仁等(2003)认为,在现有技术和应用中压碎法较高效,但受到提取率不高的影响(<80%)需要进行多次压碎;分段加热取样容易受到杂质气体的干扰,对样品纯净度要求高;激光熔蚀法每次提取的样品量很有限,要求纯化和测试系统具有较高灵敏度,比较适合丰度较高的 Ar 同位素的测量。

2 稀有气体同位素在成矿流体示踪中的应用进展

由于稀有气体同位素在不同来源地质体的组成差异很大,因此,稀有气体同位素特别是 He 和 Ar 同位素在研究成矿流体来源、演化和壳-幔相互作用过程中具有非常重要的意义。He、Ar 同位素组成在大气降水、地幔和地壳中极不相同,尤其是 $^{3}He/^{4}He$ 比值在地壳(0.01 ~ 0.05Ra, O'Nions and Oxburgh, 1983)和地幔(6 ~ 9Ra, Gautheron and Moreira, 2002; Graham, 2002)具有高达近 1000 倍的差异,即使地壳流体中有少量幔源氦的加入,氦同位素也很容易判别出来,因此,稀有气体同位素被作为幔源组分最灵敏的示踪剂,在研究成矿流体来源及壳-幔相互作用中发挥了重要作用。地质流体的 He、Ar 同位素、卤素组成不仅与流体源区相关,还与所经历的地质演化过程有关,因此,地质流体的 $^{3}He/^{4}He$、$^{40}Ar/^{36}Ar$、Br/Cl 和 I/Cl 比值可以用来指示流体和盐度源区、水-岩反应的程度和温度、流体在含水岩层中滞留的时间以及有机组分的参与等(Kendrick and Burnard, 2013)。^{3}He/热的研究可以追溯流体的热源及其运移方式等。

2.1 示踪成矿流体来源及演化

稀有气体同位素地球化学研究中最令人瞩目的进展之一,是示踪现代地热流体、天然气和成矿古流体的来源、运移机制、演化历史等,特别是壳-幔相互作用与成矿的关系方面起着越来越重要的作用。由于 He、Ar 同位素组成在地壳与地幔中极不相同,因而是壳-幔相互作用过程极灵敏的示踪剂。20 世纪末这一示踪手段引入到成矿古流体的研究中(Simmons *et al.*, 1987; Stuart and Turner, 1992; Stuart *et al.*, 1995; Burnard *et al.*, 1999; 胡瑞忠等, 1999; Hu *et al.*, 1998a, c, 2012)。迄今为止已对多种矿床类型进行了稀有气体同位素研究,包括洋中脊热液硫化物、斑岩矿床、岩浆热液矿床、矽卡岩矿床、造山带型金矿、MVT 型 Pb-Zn 矿床等。研究结果发现,除了金顶 Pb-Zn 矿(Hu *et al.*, 1998b; Tang *et al.*, 2017)以外,其他沉积岩容矿的 Pb-Zn 矿床(Kendrick *et al.*, 2002, 2005; Sánchez *et al.*, 2010; Davidheiser-Kroll *et al.*, 2014)和部分造山带或热液金矿(Pettk *et al.*, 1997; Graupner *et al.*, 2006; Morelli *et al.*, 2007)具有 <0.3Ra 但高于地壳的 $^{3}He/^{4}He$ 比值,其他类型矿床成矿流体中都具有明显的幔源流体信息(图 2, Wu *et al.*, 2018a)。

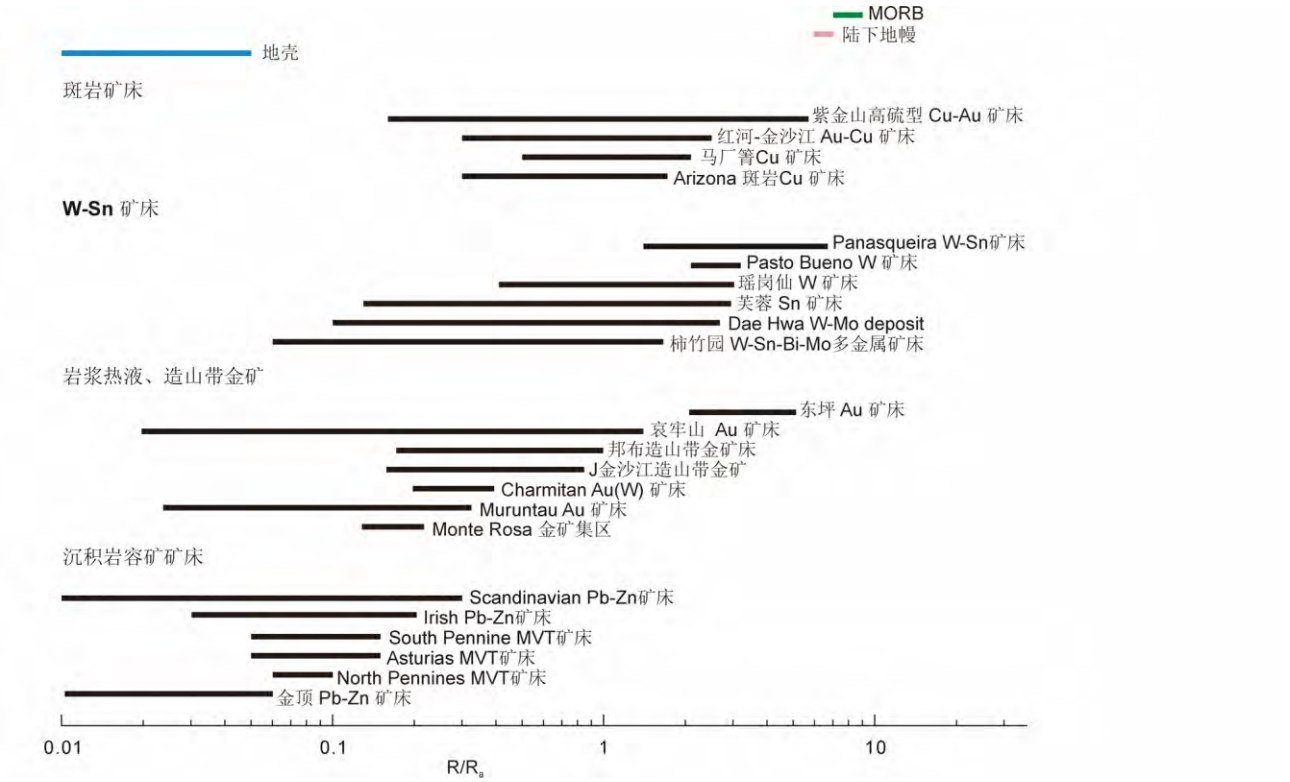

图 2 不同类型矿床成矿流体$^3He/^4He$组成(据 Wu *et al.*, 2018)

Fig. 2 $^3He/^4He$ ratio of different types of ore deposits (after Wu *et al.*, 2018)

2.1.1 洋中脊热液硫化物

自从 Turner and Stuart (1992) 对东太平洋 21°N 沉积硫化物的 He、Ar 及 Kr 同位素组成进行了研究,得出与喷口流体极其相似的同位素组成后,Turner 等就认为可以通过古代洋底沉积物来代替喷口流体样品进行$^3He/^4He$及 He/热比值的研究,这对解决洋中脊热液流体的来源、演化和热液通量等问题有着重要的意义。后来 Stuart *et al.* (1994b) 分别对中大西洋的 TAG (26°N)、Snake Pit (23°N)、东太平洋 21°N 和 Juan de Fuca 洋脊热水沉积物样品,Jean-Baptiste and FouquET (1996) 对东太平洋 13°N 热水沉积物样品,Zeng *et al.* (2001) 对大西洋中脊 TAG 热液区硫化物以及李小虎等(2014) 对西南印度洋中脊热液硫化物的 He、Ne、Ar 同位素组成进行了研究,结果显示洋中脊热液体系样品包裹体中的稀有气体是地幔和海水端元混合的产物,He 主要来自上地幔,而 Juan de Fu-ca 和西南印度洋中脊热液硫化物中有放射成因 He 的混入(Stuart *et al.*, 1994b; 李小虎等, 2014)。

2.1.2 W-Sn 矿床

华南是我国乃至全球重要的钨、锡成矿带,分布有一系列大型、超大型的矿床,如江西的西华山钨矿、大吉山钨矿、漂塘钨矿,广东的锯坂坑钨矿、瑶岭-梅子窝钨矿,湖南的芙蓉锡矿、荷花坪锡多金属矿、瑶岗仙钨矿、柿竹园钨锡多金属矿等。自 20 世纪 80 年代以来大量研究认为这些矿床大多与燕山期的陆壳重熔型或 S 型花岗岩密切相关(徐克勤等, 1984; 卢焕章, 1986; Hua *et al.*, 2003; 陈俊等, 2008),即与成矿作用密切相关的成矿流体来自壳源。然而,近年来的研究发现这些矿床成矿流体中都有不同程度幔源流体参与(Li *et al.*, 2006, 2007; 单强等, 2014; Wang *et al.*, 2010; Wu *et al.*, 2011; Hu *et al.*, 2012; Zhai *et al.*, 2012; 蔡明海等, 2012, 2013; Wei *et al.*, 2018),如图 3 所示。研究认为,华南中生代(约 150~160Ma)大规模的 W、Sn 成矿作用是壳-幔相互作用的结果。无独有偶,葡萄牙 Panasqueira W-Cu(Ag)-Sn 矿床同样也是与 S 型花岗岩有关,然而其成矿流体却具有 >5Ra的$^3He/^4He$比值,显示成矿流体中 90% 以上的 He 来自地幔(Burnard and Polya, 2004)。幔源流体如何参与到与 S 型花岗岩有关的 W、Sn 成矿作用过程? Hu *et al.* (2012) 认为与成矿有关的幔源稀有气体来自岩浆,且该岩浆由幔源岩浆底侵引起地壳物质重熔,从而使幔源 He 受到地壳放射成因^4He的影响,使得岩浆流体具有比地幔低的$^3He/^4He$值;而 Burnard and Polya (2004) 认为与花岗岩相伴的热液矿床中存在的幔源稀有气体并非来自花岗岩浆,而可能是受构造控制直接来自地幔。

2.1.3 U 矿床

华南是我国重要的铀矿资源产地,且铀矿石主要呈脉型(陈肇博, 1985)。以往研究认为这些铀矿成矿流体主要为大气降水,且铀主要来自富 U 的地壳岩石,但成矿流体中气体组分的来源及与成矿的关系尚不清楚。Hu *et al.* (2009)

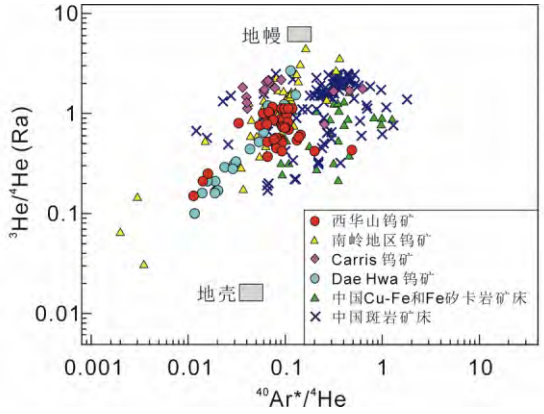

图3 W 矿和斑岩矿床成矿流体的壳-幔混合特征(据 Wei *et al.*，2018)

Fig. 3 The crust and mantle mixing characteristics of ore-forming fluid in W deposits and porphyry deposits (after Wei *et al.*, 2018)

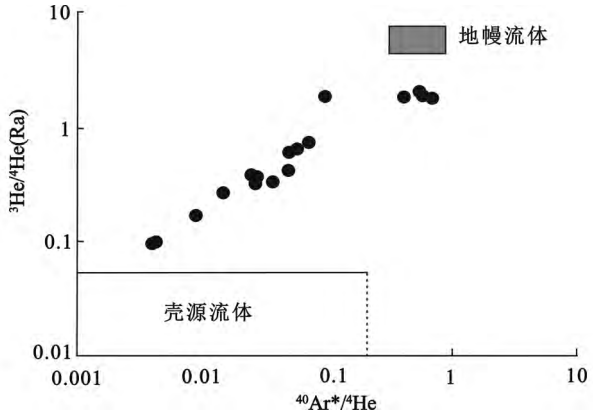

图4 相山铀矿床成矿流体的壳-幔混合特征(据 Hu *et al.*，2009)

Fig. 4 The crust and mantle mixing characteristics of ore-forming fluid in Xiangshan U deposit (after Hu *et al.*, 2009)

对华南相山铀矿成矿流体的 He、Ar 和 C 同位素进行了研究，结果表明成矿流体是富^3He 和 CO_2 的幔源流体与不含 CO_2 的大气水的混合(图4)。这些流体很有可能是白垩纪伸展和镁铁质岩墙侵入有关，地幔富 CO_2 的流体活化酸性火山岩围岩中的 U，导致 U 矿沉淀。并结合其他十几个华南代表性铀矿的 C 同位素组成和流体包裹体特征提出了华南铀矿成矿模型(Hu *et al.*，2008)，认为铀成矿与白垩纪到第三纪的地壳伸展与丰富的镁铁质岩脉的侵入和地幔源 CO_2 的向上迁移有关。在断层系统中，幔源 CO_2 进入大气成因地下水形成了富二氧化碳的热液流体。镁铁质岩浆侵入带来的热引起富 CO_2 流体在断层系统循环，并从富 U 的围岩中活化 U，以 $UO_2(CO_3)_2^{2-}$ 和 $UO_2(CO_3)_3^{4-}$ 的形式迁移。虽然温度、压力、pH 值和 Eh 值的改变可能诱发了 U 的沉淀，但流体减压和 CO_2 沸腾导致碳酸铀酰络合物的分解却是很多矿床 U 沉淀的一个关键因素在。在该模型中，地壳的幕式伸展、地幔岩浆作用和 CO_2 的释放控制着 U 的幕式成矿。

2.1.4 沉积岩容矿矿床

以沉积岩为容矿围岩的 Pb、Zn、Ag、Sb 等矿床种类繁多，储量巨大，是世界上 Pb、Zn、Ag、Sb 等资源的主要来源。传统的盆地卤水成因模型认为，成矿流体的$^3He/^4He$ 比值应该具有壳源特征。如我国规模最大的金顶 Pb-Zn 矿床，其成矿流体主要为壳源流体通过水岩反应从盆地地层中获取 S 和 Cl，以及放射成因 He 和 Ar，并从盆地底部幔源火成岩中浸取 Pb 和 Zn(Hu *et al.*，1998b; Tang *et al.*，2017)。然而，更多的矿床成矿流体中显示了地幔 He 的信息，如美国 South Pennine MVT 型矿床(Kendrick *et al.*，2002)，Scandinavian Pb-Zn 矿床(Kendrick *et al.*，2005)，西班牙北部 Asturias MVT 型 F-Ba(Zn-Pb)矿床(Sánchez *et al.*，2010)和 Irish Pb-Zn 矿(Davidheiser-Kroll *et al.*，2014)。另外，对我国华南低温成矿域中晴隆锑矿成矿流体的 He、Ar 同位素研究，结果也显示成矿流体中含有地幔流体，而含地幔 He 的流体，很可能来自右江盆地深部侏罗纪壳-幔混合成因的花岗岩浆，与华夏地块侏罗纪与钨锡成矿有关的花岗岩形成机制类似(陈娴等，2016)。

2.1.5 斑岩及其浅成热液矿床

斑岩-浅成低温热液成矿系统的研究发现，斑岩矿床及其相关的高硫型、中硫型、低硫型浅成热液矿床成矿流体的 He、Ar 同位素组成都具有壳-幔混合的特征。Hu *et al.*(1998a，c，2004)对马厂箐 Cu 矿和红河-金沙江断裂带的 Cu-Au 矿床、Kendrick *et al.*(2001a)对 6 个斑岩铜矿、Camprubí *et al.*(2006)对墨西哥 La Guitarra 中-低硫型 Ag-Au 矿床以及 Desanois *et al.*(2018)对阿根廷西北部的 Pirquitas 浅成热液 Sn-Ag-(Zn)矿床的稀有气体同位素研究结果显示，成矿流体均具有岩浆流体、地壳流体与大气降水混合特征。Manning and Hofstra(2017)对美国西南内达华州 Goldfield 和 Tonopah 浅成热液 Au-Ag 矿床以及 Wu *et al.*(2018a)对紫金山高硫型 Cu-Au 矿床稀有气体同位素研究结果显示，这些矿床的成矿流体均具有很高的$^3He/^4He$ 比值，分别为 0.05～35.8Ra 和 0.41～5.67Ra，均指示了幔源镁铁质岩浆对成矿的重要贡献，与 Hattori andKeith(2001)提出的镁铁质岩浆在斑岩矿床的形成中起着重要作用的假设是一致的。

2.1.6 华北克拉通内部金矿

华北克拉通是我国最重要的金成矿省，也是世界上重要的黄金产地之一，探明储量为 2500 吨 Au(Yang *et al.*，2003)，主要分布在华北克拉通的东缘、南缘和北缘，包括辽东-吉南、胶东、小秦岭-熊耳山、太行山中段、冀北-冀东和赤峰-朝阳等数个金矿集区(Yang *et al.*，2003)。虽然前人已做过大量研究，但对其成因和构造背景尚存争议(Hart *et al.*，2002; Mao *et al.*，2002; Yang *et al.*，2003; 翟明国等，2004; Goldfarb *et al.*，2007; Chen *et al.*，2008; 蒋少勇等，2009)。

近年来随着人们对不同矿床稀有气体同位素的研究(张连昌等,2002; Mao *et al.*,2003; 王宝德等,2003; Zhang *et al.*,2008; Li *et al.*,2012; Zhu *et al.*,2013; Tan *et al.*,2018),发现这些矿床成矿流体中都有不同程度幔源流体参与,是伸展背景下与岩石圈减薄、地幔物质上涌引起的壳-幔源长英质和镁铁质岩浆有关(Zhang *et al.*,2008; Li *et al.*,2012; Zhu *et al.*,2013; Tan *et al.*,2018);认为华北克拉通早白垩世金矿床不属于"造山型",而是"克拉通破坏型",与古西太平洋板块俯冲、回转与后撤、在地幔过渡带的滞留引起的克拉通破坏有关(Zhu *et al.*,2015)。

2.2 稀有气体同位素与卤素示踪成矿流体

卤素(Cl、Br、I)与惰性气体一样为不相容元素,其比值在不同储库中具有数量级的差异(Kendrick and Burnard,2013)。研究表明,沉积建造水中 Cl 的含量最高,Br 次之,而且 Cl、Br、F 可能受同样的地质因素制约,而 I 的制约因素则不同,I 的富集与有机质有关(Worden,1996)。Br/Cl 和 I/Cl 的比值可以有效地区分原始岩浆水、海水和沉积建造水的成分(Kendrick *et al.*,2001a)。因此,同时测量卤素与惰性气体不仅可以示踪流体来源,而且可以示踪流体盐度的来源和有机组分的参与(Böhlke and Irwin,1992b; Graupner *et al.*,2006; Kendrick *et al.*,2011b; Richard *et al.*,2014)。

目前已开展过稀有气体和卤素研究的矿床类型主要有斑岩 Cu/Cu-Mo 矿(Irwin and Roedder,1995; Kendrick *et al.*,2001a)、密西西比河谷型矿床(Böhlke and Irwin,1992a; Kendrick *et al.*,2002)、Pb-Zn 矿(Kendrick *et al.*,2005,2011b)、金矿(Graupner *et al.*,2006; Kendrick *et al.*,2011a)、Fe 氧化物 Cu-Au 矿(Kendrick *et al.*,2007)、不整合面型 U 矿(Richard *et al.*,2014)等。研究表明大多数斑岩铜矿床含有 Br/Cl 和 I/Cl 的变化范围都不大,与地幔金刚石流体包裹体的比值一致,反映了斑岩铜矿中的盐度具有初生水的来源(Irwin and Roedder,1995; Kendrick *et al.*,2001a),Silverbell 矿床高的 I/Cl 比值表明沉积建造水的参与,而 Bingham Canyon 矿床钾化带低^{36}Ar含量,高 Cl/^{36}Ar,低$^{40}Ar_E$/Cl 和高分异的$^{84}Kr/^{36}Ar$,$^{129}Xe/^{36}Ar$暗示流体发生了沸腾作用,这得到了流体包裹体数据的证实(Kendrick *et al.*,2001a)。斑岩铜矿成矿流体是低盐度,与围岩进行水-岩反应并获得放射成因^{40}Ar和卤素的饱和空气大气降水与高盐度、具有地幔流体和地壳流体混合特征的岩浆流体混合作用的结果(Irwin and Roedder,1995; Kendrick *et al.*,2001a)。大多数的 MVT 矿床具有比海水高的 Br/Cl 比值,其卤素和稀有气体同位素组成表明,MVT 矿床成矿流体具有海水蒸发与沉积孔隙水混合的特征,而且不同阶段成矿流体变化具有系统性(Böhlke and Irwin,1992a; Kendrick *et al.*,2002)。Kendrick *et al.*(2011b)对澳大利亚 Lennard Shelf Zn-Pb 矿床的卤素和稀有气体同位素研究结果显示,与矿化有关的流体包裹体的盐度和烃类含量不同,结合卤素和稀有气体同位素数据显示成矿流体为三种流体的混合。此外,根据 Br/Cl,I/Cl 和$^{40}Ar/^{36}Ar$比值的变化认为烃类和卤素分别来自沉积盆地的不同部位,证实了卤素和惰性气体示踪体系的互补性。Kendrick *et al.*(2011a)对澳大利亚西部 St Ives 金矿研究表明,稀有气体和卤素在富含 CH_4 和 H_2O-CO_2 的流体包裹体中组成不同,含 H_2O-CO_2 的流体包裹体具有高的 Br/Cl、I/Cl 值和低的放射成因稀有气体同位素,而富含 CH_4 的流体包裹体含有最高的$^{40}Ar/^{36}Ar$和$^{21}Ne/^{22}Ne$值。他们认为高的放射性成因稀有气体同位素可能由古老的基底岩石生成。稀有气体和卤素联合运用得出富含 CH_4 和 H_2O-CO_2 的流体混合引起的氧化还原反应是引起金成矿的主要原因。Richard *et al.*(2014)对加拿大 Athabasca 盆地的不整合面型 U 矿床的研究表明,Br/Cl 和 I/Cl 比值显示具有海水蒸发特征,低的 I/Cl 比值表明成矿流体未经历与有机质相互作用的过程,而$^{40}Ar/^{36}Ar$为上地壳沉积建造水特征,结合$^{84}Kr/^{36}Ar$及$^{129}Xe/^{36}Ar$组成,指出该矿床成矿流体主要为与沉积岩进行了水-岩反应的大气降水,并获得了大量放射成因^{40}Ar。因此认为成矿作用主要受蒸发和水-岩相互作用的控制。

总之,稀有气体同位素和卤素分析已被认为是示踪矿床流体来源的有力工具,为成矿流体来源、演化、矿化过程提供了新的约束,也为沉积、岩浆和变质等不同环境下矿床的形成提供了重要新认识。这些技术有望为更多其它环境下的地质过程研究提供新的视角。

2.3 ^3He/热的应用

幔源岩浆会以恒定的比例同时传输 He 和热到洋壳(Baker and Lupton,1990; Lupton *et al.*,1995; Jean-Baptiste *et al.*,1998),因此,大洋中脊流体具有^3He/热值为 $0.1\times10^{-12}\sim0.2\times10^{-12}$ cm^3 STP J^{-1}(Baker and Lupton,1990; Lupton *et al.*,1989)。另外,^3He/热记录了热如何从地幔运输到地壳的重要信息(Baker and Lupton,1990),高^3He/热值倾向于对流传递,而低^3He/热值倾向于传导传递(Baker and Lupton,1990; Turner and Stuart,1992)。因此,稀有气体同位素及^3He/热对研究成矿流体来源及热与物质传输方式具有重要意义。

Turner and Stuart(1992)首先对东太平洋隆 21°N 硫化物流体包裹体中的稀有气体同位素和^3He/热进行了研究,结果显示,^3He/热比值(1.5×10^{-13} cm^{3}STP J^{-1})与现代喷口流体的^3He/热比值(1×10^{-13} cm^{3}STP J^{-1}, Lupton *et al.*,1980)基本一致。因此,认为流体包裹体中的^3He/热比值可用于地壳成矿古流体系统的研究。

Burnard *et al.*(1999)研究发现中国云南哀牢山金成矿带大坪金矿的^3He/热比值($0.7\times10^{-12}\sim37\times10^{-12}$ cm^3 STP J^{-1})远远大于墨江金矿和镇沅金矿的^3He/热比值($0.1\times10^{-12}\sim0.8\times10^{-12}$ cm^3 STP J^{-1}),指出大坪金矿的形成与岩浆流体的直接注入有关,而墨江金矿和镇沅金矿的形成可能是岩浆流体与其他流体混合作用的结果。Burnard and Polay

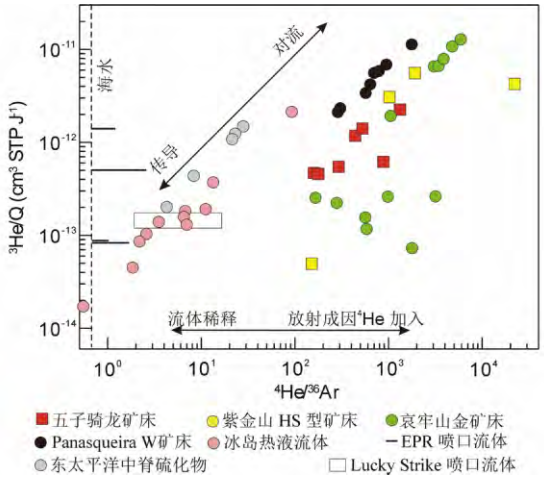

图 5 不同矿床成矿流体及喷口流体的$^{3}He/Q$–$^{4}He/^{36}Ar$图

Fig. 5 $^{3}He/Q$ vs. $^{4}He/^{36}Ar$ from deposits and vent fluids

(2004)对葡萄牙中部的 Panasqueira W-Cu(Ag)-Sn 矿床的研究结果表明，成矿流体的$^{3}He/^{4}He$(>5Ra)和^{3}He/热值非常高($1\times10^{-12}\sim10\times10^{-12}cm^{3}$ STP J^{-1})，由侵入体的逐渐冷却为成矿系统提供热似乎不太可能，He 和热可能都来自地幔，而且 He 和热是通过对流方式进入成矿流体。我国福建紫金山 Cu-Au-Mo-Ag 矿田成矿流体的也具有高的^{3}He/热值($0.07\times10^{-12}\sim8.35\times10^{-12}cm^{3}$ STP J^{-1})，与 Panasqueira W-Cu(Ag)-Sn 矿床值相近(图 5)，这种高的$^{3}He/^{4}He$和^{3}He/热值暗示成矿流体的挥发分和热可能直接来自底侵的镁铁质岩浆，而且挥发分和热以对流方式进入成矿系统(Wu *et al.*，2018a)。

以上研究^{3}He/热值都是基于$^{3}He/^{36}Ar$值计算，而 Zeng *et al.*(2015)用$^{3}He/^{22}Ne$和$^{4}He/^{20}Ne$值计算了东太平洋隆、中大西洋脊、中印度洋脊、西南印度洋脊、北斐济后弧形盆地的硫化物矿床成矿流体的^{3}He/热和^{4}He/热值，结果表明，^{3}He/热值为$0.22\times10^{-14}\sim3.44\times10^{-14}cm^{3}$ STP J^{-1}，^{4}He/热比值为$0.17\times10^{-9}\sim3.13\times10^{-9}cm^{3}$ STP J^{-1}，与东太平洋隆 13°N，1～2°S 的^{3}He/热($0.36\times10^{-14}\sim3.44\times10^{-14}cm^{3}$ STP J^{-1})和^{4}He/热($0.32\times10^{-9}\sim3.13\times10^{-9}cm^{3}$ STP J^{-1})值一致，并根据全球高温热液喷气口 He 和热流值推算大概 3% 的大洋热由洋底高温热液活动提供。

^{3}He/热在矿床中的研究还处于起步阶段，已研究的矿床类型和数量都有限，尚需开展更多的工作，以促进成岩、成矿过程中热机制研究。

3 年代学研究

同位素测年是地质测年的主要手段，稀有气体同位素测年为其重要分支，其放射性纪年被记录在 He、Ne、Ar、Kr、Xe 等同位素中。近年来，流体包裹体^{40}Ar–^{39}Ar、表生含钾矿物的^{40}K–^{40}Ar、^{40}Ar–^{39}Ar定年和(U-Th)/He 热年代学在矿床年代学研究中取得重要进展。高精度的^{40}Ar–^{39}Ar计时技术的建立，使流体包裹体^{40}Ar–^{39}Ar定年成为可能；由于激光加热技术的发展，Ar-Ar 法用于表生含钾矿物、年轻样品的直接定年；而基于不同矿物对 He 的不同封闭温度(U-Th)/He 测年技术主要用于揭示矿床的隆升、剥露历史以及原生、次生赤铁矿定年等。含钾矿物的^{40}K–^{40}Ar、^{40}Ar–^{39}Ar定年以及(U-Th)/He 定年为矿床及氧化带的形成时间、构造隆升、古气候演化等重大地质问题的讨论提供了大量有意义的信息。

3.1 流体包裹体 Ar-Ar 定年技术在矿床成矿年龄中的应用

近年来对金属矿床直接定年的方法取得了很大进展，然而，对大多数矿床来说，要准确测定其成矿年龄还存在一定的困难。对于许多金属矿床，由于难以找到既能够代表成矿时代、同时又适合于常规同位素定年方法的测定对象，难以对其进行直接定年。Re-Os 和 La-Ce 法适用面很窄，只有少数的特殊矿物可作为测定对象，Rb-Sr、Sm-Nd 和 Pb-Pb 等时线法常因一组样品同位素组成相近而不能构成等时线(邱华宁等，1997)。热液矿床中矿物通常含有较丰富的流体包裹体，其中存在着一定量的钾，因此，流体包裹体$^{40}Ar/^{39}Ar$测年方法便应运而生了。

Kelley *et al.*(1986)首先利用真空压碎技术对石英流体包裹体^{40}Ar–^{39}Ar法定年进行了尝试，但因样品中含大量的过剩^{40}Ar，且放射成因^{40}Ar比例太低而未获得满意的年龄数据。Turner and Wang(1992)采用^{40}Ar–^{39}Ar真空击碎技术和阶段加热技术分析了河北省蓟县中元古长城系大红峪组燧石(JX04)和山西省五台地区滹沱群东冶亚群纹山组燧石叠层石(WT03)，获得了有意义的年龄结果。Qiu ang Dai(1989)特别设计了全金属超高真空碎样装置，该装置与 MM-1200 质谱计的纯化系统直接相连，以真空破碎方法提取流体包裹体，成功测定了滇西泸水钨锡矿床石英的年龄(邱华宁等，1994)。其后又测定了滇西腾冲上芒岗金矿(Qiu，1996)、东川铜矿(邱华宁等，1997，2000，2001，2002；Qiu *et al.*，2002)、大兴安岭北部砂宝斯金矿床(刘军等，2013)、柿竹园多金属矿(王敏等，2016)等矿床的石英流体包裹体的年龄，获得了与地质事实相吻合的成矿年龄数据。随后又开展了石榴石(邱华宁等，2004；Qiu and Wijbrans，2006，2008)、闪石(邱华宁和 Wijbrans，2006；邱华宁等，2009；Qiu *et al.*，2010a；胡荣国等，2013；Hu *et al.*，2015，2016)、锡石(白秀娟等，2011，Bai *et al.*，2013；王敏等，2015)和黑钨矿(Bai *et al.*，2013)等矿物的流体包裹体^{40}Ar–^{39}Ar定年，均获得很好的实验结果，获得了与地质事实相吻合的成矿年龄数据。

由于硫化物经中子活化后具有高放射性、而且硫化物加热熔化后会产生含硫的气体，对质谱系统有害及实验后样品粉末难于处理等原因，使得对其流体包裹体^{40}Ar–^{39}Ar定年研究工作较少。直到 20 世纪 80 年代初，人们才开始对硫化物$^{40}Ar/^{39}Ar$定年的探索。首先，York *et al.*(1982)对黄铁矿

作了全熔$^{40}Ar/^{39}Ar$定年研究,指出尽管黄铁矿的钾含量很低,但仍不失为硫化物矿床直接定年的合适对象。范才云等(1986)采用阶段加热法做了黄铁矿的^{40}Ar–^{39}Ar年代学的研究,表明黄铁矿可以作为该方法的分析对象,并指出开展其它硫化物的^{40}Ar–^{39}Ar定年研究具有重要的意义。后来,Smith *et al.*(2001, 2005)及Phillips and Miller(2006)分别采用激光探针技术对单颗粒的黄铁矿进行了^{40}Ar–^{39}Ar定年研究,获得了有意义的年龄数据,研究表明具有一定钾含量的硫化物可能进行^{40}Ar–^{39}Ar定年,同时指出该方法是一种有效的直接测定黄铁矿年龄的方法。随后,邱华宁的团队(Qiu and Jiang, 2007; Jiang *et al.*, 2012; 蒋映德等, 2007)开展了闪锌矿真空压碎和阶段加热^{40}Ar–^{39}Ar定年,获得一致的原生包裹体年龄和闪锌矿中钾矿物微晶年龄,为硫化物矿床直接定年提供了新的技术手段。

3.2 表生环境中含K矿物K–Ar和激光$^{40}Ar/^{39}Ar$定年

由于风化作用一般都在较为开放的体系中进行,同时在风化剖面中很难获得适合常规定年方法的次生矿物,因此,风化剖面的直接定年一直是该领域的科学难题之一。这主要是,长期以来,风化壳测年的研究一般都基于风化壳与其上、下地质体(年龄已知)的相对层序来间接确定(Bird, 1989),这在多数情况下不能给出准确的风化壳年龄。尽管如此,各国科学家一直在寻找直接对风化剖面测年的方法,较成功的有古地磁法、风化速率法和同位素法。近年来利用放射性同位素定年的一个重要进展是含钾矿物K–Ar和激光$^{40}Ar/^{39}Ar$定年。

早在20世纪60年代,苏联学者Chukhrov *et al.*(1969)就利用表生过程中形成的明矾石族矿物进行了风化壳测年,尝试解决风化壳及与其相关的年代学问题。但由于K–Ar定年方法本身的局限性,如所需样品量大、不能有效识别样品中可能存在的过剩氩、原生矿物及多期矿物共存的现象,以及风化产物中复杂的矿物组成及共生次序、矿物晶体细小等原因,难以获得大量纯净的、完全不受原生矿物影响的定年矿物,使得该方法研究没有取得实质性进展。直到20世纪90年代,Vasconcelos *et al.*(1992, 1994a, b)的研究小组开始使用激光$^{40}Ar/^{39}Ar$技术对明矾石和黄钾铁矾矿物进行定年,才使得风化年代学研究获得突破性进展。激光熔样方法引入$^{40}Ar/^{39}Ar$定年,不仅减少了样品的用量,同时也降低了系统的空白本底水平;利用阶段加热法得到的年龄谱图,不仅可以有效识别原生矿物的混染和多世代矿物的存在,还可以检测样品中的过剩/继承Ar(杨静等, 2013)。激光$^{40}Ar/^{39}Ar$定年法一个很重要的应用就是可以对单个晶体进行$^{40}Ar/^{39}Ar$定年,这种单晶定年方法使风化壳中少量存在的明矾石、黄钾铁矾和含钾锰矿物等含钾矿物定年成为可能(Vasconcelos *et al.*, 1994a, b; Ruffet *et al.*, 1996; Vasconcelos, 1999),随之开启了表生年代学研究的新热潮。

Vasconcelos *et al.*(1994a)首次对美国内达华州Goldfield矿表生明矾石和黄钾铁矾进行了$^{40}Ar/^{39}Ar$定年,表明美国西部普遍深入的风化作用发生于晚中新世(大约10Ma),这个结果与Ashley and Silberman(1976)报道的表生明矾石K–Ar年龄的研究结果一致。Vasconcelos and Conroy(2003)将同一个黄钾铁矾样品的3个颗粒,分别进行了$^{40}Ar/^{39}Ar$年龄测定,结果得到非常一致的坪年龄(分别为0.92±0.03Ma、0.96±0.02Ma、0.89±0.06Ma)和反等时线年龄(0.99±0.03Ma)。他对明矾石样品进行了类似的研究也得到了一致的坪年龄和反等时线年龄。这表明表生黄钾铁矾和明矾石可以很好的保存Ar,适合表生年龄定年。而且,Vasconcelos and Conroy(2003)对同一个黄钾铁矾样品中细晶质颗粒(粒径<10μm)和粗晶质颗粒(粒径>100μm)分别进行了年龄测定,得到了几乎相同的坪年龄,表明无论粒度大小,黄钾铁矾都可以很好地保存Ar,适合表生年龄定年。Vasconcelos *et al.*(1992)对巴西Minas Gerais地区一个风化成因的隐钾锰矿进行了激光$^{40}Ar/^{39}Ar$年代学研究,获得9.94±0.05Ma和5.59±0.10Ma的年龄,认为这个年龄体现了风化过程发生的时间,指示该区甚至整个南美大陆在晚中新世时为温暖潮湿的气候。Vasconcelos *et al.*(1994b)和Ruffet *et al.*(1996)分别对巴西Carajàs地区风化壳中锰的氧化物进行了激光$^{40}Ar/^{39}Ar$定年,结果表明K–Mn氧化物可以很好的保存Ar,而且认为K–Mn氧化物的生长是一个连续的过程(Ruffet *et al.*, 1996)而非幕式生长(Vasconcelos *et al.*, 1994b)。De Putter *et al.*(2015)对非洲刚果的Kisenge锰矿次生富集产生的隐钾锰矿进行了$^{40}Ar/^{39}Ar$定年,结果显示风化年龄随着深度降低而变年轻,并推断这可能与东非地台的抬升和随后东非大裂谷的形成有关。Bonnet *et al.*(2016)对印度半岛西部沿海的低地和东部高原的高地的含锰红土剖面进行了钾锰氧化物的$^{40}Ar/^{39}Ar$定年,分别获得了53~50Ma、37~23Ma(高地)和47~45Ma、24~19Ma、9Ma、2.5Ma(低地)不同的风化年龄,发现53~45Ma时高地和低地都出现了红土风化,强烈的风化作用记录了气候变化和季风的影响,同时记录了始新世之后低地和高地的不同侵蚀和风化历史。对南美洲的Atacama沙漠和秘鲁地区不同矿床中的风化矿物的K–Ar和$^{40}Ar/^{39}Ar$定年研究表明南美Atacama沙漠地区大量明矾石族矿物的年龄主要集中在早中新世至中中新世(距今9~24Ma),中中新世后明矾石族矿物生成逐渐减少,这些结果表明Atacama沙漠地区早中新世到中中新世的干旱-半干旱气候逐渐被晚中新世极干旱气候所取代(Sillitoe and McKee, 1996; Mote *et al.*, 2001; Bouzari and Clark, 2002; Quang *et al.*, 2003, 2005; Arancibia *et al.*, 2006)。

在国内,风化壳含钾矿物的K–Ar和^{40}Ar–^{39}Ar定年研究虽然才刚刚起步,但已经取得很好的研究成果。如许英霞等(2008)和何为等(2009)分别尝试用K–Ar法对氧化带中的绿钾铁矾、高铁叶绿矾、绿钾铁矾和黄钾铁矾等含钾硫酸盐进行了定年,获得东天山红山高硫型铜金矿床60~3.7Ma的表生年龄。Li *et al.*(2002)和李建威等(2004)对钾锰矿物激

光^{40}Ar-^{39}Ar方法和意义进行了综述；杨静等(2013，2015)分别对明矾石组矿物和黄钾铁矾的激光^{40}Ar-^{39}Ar定年方法及样品采集、制备等进行了详细的介绍。Chen and Li (2014)对青藏高原东北缘祁连山地区白银矿田折腰山块状硫化物矿床风化壳中两种产状的表生黄钾铁矾进行了$^{40}Ar/^{39}Ar$和H-O同位素地球化学研究，分别获得41.2±0.4Ma与37.1±0.3Ma和3.3±0.1Ma与3.2±0.1Ma的$^{40}Ar/^{39}Ar$年龄，对应的δD值分别为156‰和133‰，及160‰和158‰，表明白银矿田折腰山矿床至少在始新世中期就已隆升到地表，并接受了长期的化学风化和矿床的次生富集，其中，晚始新世和晚上新世的2次风化事件记录了白银地区干旱半干旱气候条件下2次相对湿润的气候，年代学为该区硫化物矿床的化学风化和次生富集提供了直接的年龄限定。Deng *et al.* (2014)对云南巴夜锰矿风化剖面的钾锰氧化物进行了激光$^{40}Ar/^{39}Ar$定年，限定了风化作用的时间以及古气候和地貌演化。Yang *et al.* (2016)对吐哈盆地中红山、硫磺山、彩华沟三个矿床风化剖面中的表生黄钾铁矾和斜钾铁矾进行了$^{40}Ar/^{39}Ar$定年，限定了其风化和表生富集作用发生的时间为33.3±0.5Ma到3.3±0.4Ma，持续了30Myr。Deng *et al.* (2016)对贵州遵义锰矿的22个氧化锰颗粒进行了$^{40}Ar/^{39}Ar$定年，得到从13.1±0.3Ma到0.1±0.4Ma的年龄，而且具有从上到下逐渐变年轻的趋势，并获得风化前锋拓展速率为3.3m/Myr，相应的化学剥蚀速率为4.6±0.2t/km^2/yr。

风化壳和矿床次生富集带的含钾矿物的K-Ar和激光$^{40}Ar/^{39}Ar$定年，不仅为查明大陆化学风化和矿床次生富集的时间和过程提供了可能，而且为地貌演化、区域古气候古环境的反演提供了新的思路和手段。

3.3 (U-Th)/He热年代学

早在二十世纪初，随着放射性的发现，人们就意识到可以用放射性成因He对矿物进行定年(Strutt，1908，1910)。在1950年代以前，(U-Th)/He定年是最重要的定年方法(Hurley and Goodman，1943)。但是由于该方法所获得年龄一般要比实际年龄偏轻，后来被K-Ar法(Wasserburg and Hayden，1955)、^{40}Ar-^{39}Ar法(Merrihue and Turner，1966)和Rb-Sr、Sm-Nd法取代。近年来，随着分析手段和实验设备的进一步提高，以及人们对矿物He封闭温度的研究和认识的深入，(U-Th)/He方法又重新得到学术界的关注。

可用于(U-Th)/He定年的矿物主要有锆石(Farley *et al.*，2002；Reiners *et al.*，2002；Dobson *et al.*，2008；Horne *et al.*，2016)、磷灰石(Wolf *et al.*，1996；Farley *et al.*，2002；Flowers *et al.*，2009)、石榴石(Aciego *et al.*，2003)、橄榄石(Aciego *et al.*，2007)、榍石(Reiners and Farley，1999；Stockli and Farley，2004；Horne *et al.*，2016)、磁铁矿(Blackburn *et al.*，2007)、针铁矿(Shuster *et al.*，2005；Monteiro *et al.*，2014；Riffel *et al.*，2015；Deng *et al.*，2017)、赤铁矿(Wernicke and Lippolt，1997a，b；Farley and Flowers，2012；Danišík *et al.*，2013)、萤石(Evans *et al.*，2005)和自然金(Shukolyukov *et al.*，2010)等。不同矿物(U-Th)/He体系的封闭温度差别较大，如果矿物的封闭温度较高并接近矿物的形成温度，则测得的年龄可代表矿物的形成年龄；如果矿物的封闭温度较低，则测定的年龄只代表达到同位素体系封闭温度时的时间。因此，(U-Th)/He定年不仅可以用于地质体定年、年轻火山岩的喷发年龄和年轻断层活动年龄研究，还可以联合使用不同矿物和同位素测年方法用于造山带演化重建，盆地热历史恢复、岩浆冷却历史、古地貌研究以及矿床隆升剥蚀等方面的研究。近年来U、Th含量较高的锆石和磷灰石研究较多，成为(U-Th)/He定年技术常用的矿物。而风化矿物赤铁矿、针铁矿和褐铁矿等铁氧化物(U-Th)/He年龄代表了矿物开始沉淀至今的时间，是风化地质年代学研究的重要手段，以下将着重对这两方面进行论述。

3.3.1 锆石、磷灰石(U-Th)/He定年

锆石以副矿物的形式广泛存在于各类岩石中，而且锆石中富含放射性元素U、Th，具有良好的抗风化能力，在岩浆作用和变质作用等热动力过程中具有基本不受影响的耐久性，使其成为用于地质年代学和热年代学研究的理想定年矿物。研究表明，对于火山岩等快速冷却的样品，锆石(U-Th)/He年龄值具有结晶年龄意义。磷灰石He封闭温度是目前已知定年体系中最低的，其可以反映其他方法难以涉及的低温范围的热事件年龄，这使人们对于该方法产生了浓厚的兴趣。研究表明磷灰石的He封闭温度为75±5℃(图6)，He的部分保存区间为85~40℃(Wolf *et al.*，1996)，锆石的He封闭温度为170~190℃，而遭受了辐射损伤的锆石的封闭温度则较低为140~160℃(Reiners *et al.*，2002)。自从Zeitler *et al.* (1987)对磷灰石进行(U-Th)/He定年时发现磷灰He年龄是通过较低温度时的冷却年龄，并指出(U-Th)/He定年有可能作为一种低温温度计之后，这项研究引起了研究人员的极大关注，从而为(U-Th)/He定年的快速发展奠定了基础。

目前国内外的研究均采用将(U-Th)/He方法与裂变径迹甚至K/Ar，Ar/Ar、U-Pb等其它同位素定年方法结合起来使用，以便利用不同矿物、不同测年方法封闭温度的不同(图6)，综合起来对复杂热史轨迹进行恢复。Reiners *et al.* (2003)利用锆石、磷灰石(U-Th)/He和磷灰石裂变径迹年龄研究了中国东部大别山约115Myr的冷却、剥露历史。Qiu *et al.* (2010b)利用塔里木盆地钻井样品的磷灰石与锆石(U-Th)/He年龄数据，结合磷灰石裂变径迹和有机质镜质体反射率等古温标模拟了塔里木盆地不同井区古生代的热历史，并计算了古生代不同时期的古地温梯度，为缺乏常规古温标的塔里木盆地下古生界碳酸盐层系所经受热史的恢复提供了新方法。许长海等(2010)在对大巴山弧形构造带形成与两侧隆起关系的研究中，利用磷灰石裂变径迹和(U-Th)/He低温热年代学方法分别分析了南大巴山弧形带的热历史，以及汉南-米仓山隆起和黄陵隆起的热历史。Harris *et al.* (2008)对阿根廷的Bajo de la Alumbrera斑岩Cu-Au矿床的

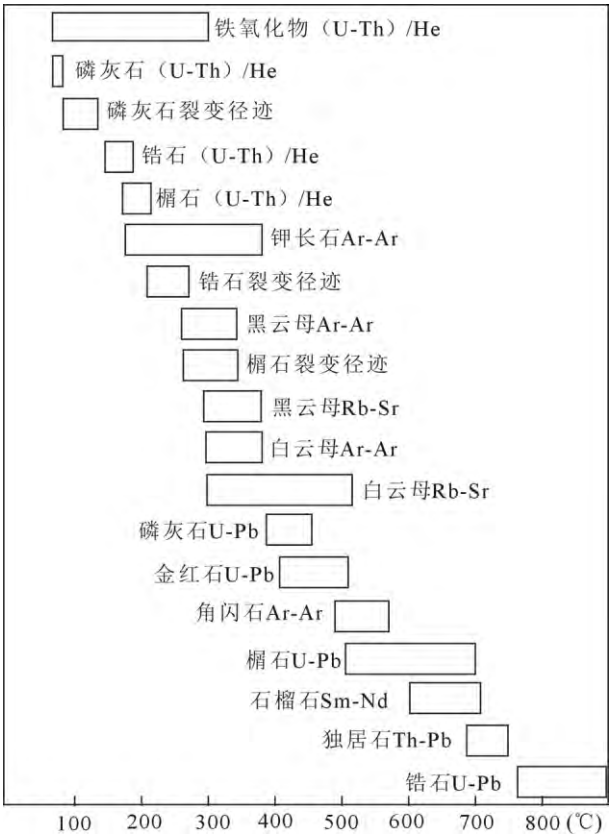

图 6 不同矿物不同同位素定年体系的封闭温度

Fig. 6 Temperature range of thermochronometers

斑岩侵入体进行了 U-Pb 和$^{40}Ar/^{39}Ar$ 年代学和锆石、磷灰石(U-Th)/He 定年，揭示了多期岩浆活动和热事件的时间，及其冷却历史。Li *et al.* (2014) 利用锆石 U-Pb，黑云母$^{40}Ar/^{39}Ar$ 和锆石、磷灰石(U-Th)/He 方法研究了包古图斑岩铜矿床的热-构造演化历史，认为大气降水的影响导致了(U-Th)/He 年龄偏老，并识别出五个阶段的冷却历史：晚石炭-早二叠世的快速冷却阶段(320～290Ma)，早二叠世-晚三叠世缓慢冷却(290～200Ma)，早侏罗世到早白垩世的极缓慢冷却阶段(200～136Ma)，早白垩世到晚白垩世(136～100Ma)的快速冷却阶段以及晚白垩世以来的十分缓慢的冷却(100Ma)；不同的冷却阶段主要是受制于欧亚大陆-羌塘地块以及羌塘地块与拉萨地块的碰撞拼合。喻顺等(2016)利用磷灰石(U-Th)/He 方法重建了中天山南缘科克苏河地区中-新生代构造热演化及隆升剥蚀过程，表明中天山南缘隆升剥蚀存在不均一性，分别在晚白垩世、早中新世、晚中新世发生了快速隆升剥蚀事件。Ershova *et al.* (2018) 对俄罗斯 High Arctic 卡拉岩层的古地理进行了研究，(U-Th)/He 年龄显示样品在沉积后没有被重置，暗示碎屑锆石携带着源区物质剥露历史信息，利用锆石(U-Th)/He 和 U-Pb 年龄反演了源区物质的剥露抬升历史。

利用矿床中常见的磷灰石、锆石矿物进行成矿后的剥蚀历史的研究已经成为矿床学的重要研究内容。但是，数据解释一定要与地质事实相结合，不然会得到错误的结论。如 Weisberg *et al.* (2018) 在对科罗拉多西部山区的麦克卢尔山正长岩进行研究时就发现如果仅根据锆石、榍石和磷灰石(U-Th)/He 年龄数据，以及 U-Pb 和$^{40}Ar/^{39}Ar$ 年龄可得出岩体经过简单的缓慢单调冷却历史，然而，此结果却与地质事实不相符；年龄数据与地质现象结合后得出岩体曾 3 次经过不同程度的埋藏和剥蚀而到达地表。

3.3.2 铁氧化物的(U-Th)/He 定年

赤铁矿、褐铁矿等形成于低温条件下，而且含有适量的 U-Th 含量，几乎不存在继承 He，为赤铁矿和镜铁矿等含铁氧化物(U-Th)/He 定年提供了可能。此技术应用的关键是赤铁矿等含铁矿物对 He 的封闭温度。Lippolt *et al.* (1993)、Bähr *et al.* (1994) 开展了一些不同粒度、不同冷却速率和不同晶型的赤铁矿 He 保存能力的实验，研究发现表生赤铁矿(10μm)在 300Myr 内^{4}He 的丢失不会超过 0.9%(Lippolt *et al.*，1993)，冷却速率为 10K/Myr 和10^{3}K/Myr，粒度为 10～500μm 时的封闭温度分别是 200℃和 300℃，冷却速率为$10K/10^{6}$ 年时镜铁矿封闭温度为 219℃，葡萄状赤铁矿封闭温度为 122℃，而且在地壳表面的热条件下针铁矿的 He 丢失不可测量，而葡萄状赤铁矿的 He 丢失可以忽略不计(<2%)(Bähr *et al.*，1994)。Evenson *et al.* (2014) 研究了多晶集合体赤铁矿和单个赤铁矿晶体中^{4}He 的扩散行为，并结合前人的实验数据，用动力学数据计算了大多数样品的封闭温度为 140～240℃。Balout *et al.* (2017) 计算了赤铁矿中^{4}He 的显微尺度三维扩散系数，结果显示赤铁矿粒度为 0.1μm 和 10μm 时的封闭温度分别为 83℃和 154℃。最近，Farley (2018) 对不同粒度的单个赤铁矿晶体的 He 扩散行为进行了研究，结果显示赤铁矿可以很好的保存 He，即便一个 20nm 的赤铁矿晶体在 30℃下 1Myr 时间里可以保存 99% 的 He，在 100Myr 里可以保存 90% 的 He；在一个冷却速率为 10℃/Myr 的系统中，20nm 的赤铁矿封闭温度为约 70℃度，跟 100μm 磷灰石相当。可见，这种技术用于风化铁矿石定年的潜力是显而易见的。

Fe 的氧化物(U-Th)/He 定年最早在 1908 年由 Strutt 报道(Strutt，1908)。后来 Fanale andKulp (1962) 给出了 Pennsylvania Cornwall 磁铁矿矿床 He 等时线年龄(194±4Ma)与共生白云母的 K-Ar 年龄一致。近年来，Wernicke 和 Lippolt 成功地用针铁矿、赤铁矿和褐铁矿(U-Th)/He 方法给出了欧洲一些矿脉年龄(Wernicke and Lippolt，1993，1994a，b，1997a，b；Lippolt *et al.*，1995，1998)，获得的年龄变化从 0.8Ma 到 180Ma。Reiner *et al.* (2015) 对前寒武纪基底基岩中次生赤铁矿进行(U-Th)/He 定年获得老至 1.6Ga 的年龄，表明在地质时间内 He 可以保存。Wu *et al.* (2018b) 利用赤铁矿(U-Th)/He 方法测定了意大利 Elba 岛热液铁矿床的成矿年龄。另外，(U-Th)/He 定年还用于研究美国 Grand Canyon 地区的热演化历史(Farley and Flowers，2012)、三叠纪古河道沉积的铁豆年龄(Danišík *et al.*，2013)、断层活动

年龄(Ault *et al.*, 2015a, b; Garcia and Reiners, 2015; McDermott *et al.*, 2015; Reiners *et al.*, 2015),甚至试图用于限定火星上水活动的时间(Kula and Baldwin, 2012)。此外,(U-Th)/He 和^{40}Ar-^{39}Ar 定年联合应用还可以对风化剖面和相关的矿化提供强有力的风化年龄和冷却历史(Riffel *et al.*, 2015)。Deng *et al.* (2017)以玉龙斑岩型铜矿床的铁帽为研究对象,对上百米厚铁帽中的针铁矿开展了系统的(U-Th)/He 年代学研究。指出风化壳年代学不仅可以揭示矿床次生氧化富集过程,而且可以作为一个重要的古气候指标。由于针铁矿、赤铁矿和褐铁矿在风化壳中广泛存在,因此,(U-Th)/He 定年在风化壳年代学研究中具有广泛的应用前景(Shuster *et al.*, 2005; Heim *et al.*, 2006)。

国内(U-Th)/He 定年技术方法刚刚起步,主要应用于磷灰石和锆石的热年代学研究,很少用于铁氧化物定年分析。但我们已经有了较好的理论基础和硬件条件。自 2007 年开始,中国科学院广州地球化学研究所、中国地质科学院地质研究所(陈文和张彦, 2010; 张彦等, 2011; 张彦和陈文, 2011; 孙敬博等, 2017)、成都地质调查中心、中国石化无锡石油地质研究所(王杰和马亮帮, 2014)、中国科学院地质与地球物理研究所(吴林等, 2016)、中国地震局地质研究所(王英等, 2017)等单位也相继建立起(U-Th)/He 实验室并逐步进行实验方法和流程的探索。这些硬件设施都为我国开展锆石、磷灰石、榍石、铁氧化物等矿物的(U-Th)/He 定年提供了条件。

4 结语与展望

随着测试水平及分析手段的发展,人们对稀有气体同位素的认识不断深入,而稀有气体同位素在矿床学研究中的应用也取得了许多重要进展。不仅揭示了不同类型矿床成矿流体的来源、演化过程、矿床沉淀机制,探讨了壳-幔相互作用在不同类型矿床成矿过程中的作用,尤其是地幔物质、挥发份与热在超大型矿床形成中的重要贡献,而且对矿床形成时间、发生表生氧化、次生富集时间的厘定、以及矿床形成后的抬升、剥露历史有了更深入的认识。然而由于稀有气体同位素本身的局限性,需要与其他同位素示踪体系联合运用才能更好地解决成矿流体来源、演化、成矿模式等方面的问题。另外,只有更好的理解稀有气体在不同矿物、不同温度下的扩散行为,才能更好地解释其年代学意义。随着人们对稀有气体同位素在岩浆-流体演化过程中的行为以及不同矿物中的扩散行为的深入认识,将大大促进稀有气体同位素在矿床学中的应用。

致谢 评审专家贺怀宇研究员和邱华宁教授对论文提出了建设性修改意见,在此深表感谢!

References

Aciego S, Kennedy BM, DePaolo DJ, Christensen JN and Hutcheon I. 2003. U-Th/He age of phenocrystic garnet from the 79 AD eruption of Mt. Vesuvius. Earth and Planetary Science Letters, 216(1-2): 209-219

Aciego SM, DePaolo DJ, Kennedy BM, Lamb MP, Sims KWW and Dietrich WE. 2007. Combining [He] cosmogenic dating with U-Th/He eruption ages using olivine in basalt. Earth and Planetary Science Letters, 25(3-4): 288-302

Arancibia G, Matthews SJ and de Arce CP. 2006. K-Ar and $^{40}Ar/^{39}Ar$ geochronology of supergene processes in the Atacama Desert, Northern Chile: Tectonic and climatic relations. Journal of the Geological Society, 163(1): 107-118

Ashley RP and Silberman ML. 1976. Direct dating of mineralization at Goldfield, Nevada, by potassium-argon and fission-track methods. Economic Geology, 71(5): 904-924

Ault AK, Frenzel M, Reiners PW, Woodcock NH and Thomson SN. 2015a. Hematite (U-Th)/He and apatite fission-track dating constrain paleofluid circulation in faults: An example from Gower Peninsula fissure fills, wales. In: American Geophysical Union, Fall Meeting 2015. Washington: AGU

Ault AK, Reiners PW, Evans JP and Thomson SN. 2015b. Linking hematite (U-Th)/He dating with the microtextural record of seismicity in the Wasatch fault damage zone, Utah, USA. Geology, 43(9): 771-774

Bähr R, Lippolt HJ and Wernicke RS. 1994. Temperature-induced ^{4}He degassing of specularite and botryoidal hematite: A ^{4}He retentivity study. Journal of Geophysical Research, 99(89): 17695-17707

Bai XJ, Wang M, Lu KH, Fang JL, Pu ZP and Qiu HN. 2011. Direct dating of cassiterite by $^{40}Ar/^{39}Ar$ progressive crushing. Chinese Science Bulletin, 56(23): 1899-1904 (in Chinese)

Bai XJ, Wang M, Jiang YD and Qiu HN. 2013. Direct dating of tin-tungsten mineralization of the Piaotang tungsten deposit, South China, by $^{40}Ar/^{39}Ar$ progressive crushing. Geochimica et Cosmochimica Acta, 114: 1-12

Bai XJ, Jiang YD, Hu RG, Gu XP and Qiu HN. 2018. Revealing mineralization and subsequent hydrothermal events: Insights from $^{40}Ar/^{39}Ar$ isochron and novel gas mixing lines of hydrothermal quartzes by progressive crushing. Chemical Geology, 483: 332-341

Baker ET and Lupton JE. 1990. Changes in submarine hydrothermal ^{3}He/heat ratios as an indicator of magmatic/tectonic activity. Nature, 346(6284): 556-558

Ballentine CJ and Burnard PG. 2002. Production, release and transport of noble gases in the continental crust. Reviews in Mineralogy and Geochemistry, 47(1): 481-538

Balout H, Roques J, Gautheron C, Tassan-Got L and Mbongo-Djimbi D. 2017. Helium diffusion in pure hematite (α-Fe_2O_3) for thermochronometric applications: A theoretical multi-scale study. Computational and Theoretical Chemistry, 1099: 21-28

Bird MI, Andrew AS, Chivas AR and Lock DE. 1989. An isotopic study of surficial alunite in Australia: I. Hydrogen and sulphur isotopes. Geochimica et Cosmochimica Acta, 53(12): 3223-3237

Blackburn TJ, Stockli DF and Walker JD. 2007. Magnetite (U-Th)/He dating and its application to the geochronology of intermediate to mafic volcanic rocks. Earth and Planetary Science Letters, 259(3-4): 360-371

Böhlke JK and Irwin JJ. 1992a. Brine history indicated by argon, krypton, chlorine, bromine, and iodine analyses of fluid inclusions from the Mississippi Valley type lead-fluorite-barite deposits at Hansonburg, New Mexico. Earth and Planetary Science Letters, 110(1-4): 51-66

Böhlke JK and Irwin JJ. 1992b. Laser microprobe analyses of Cl, Br, I, and K in fluid inclusions: Implications for sources of salinity in some ancient hydrothermal fluids. Geochimica et Cosmochimica Acta, 56

(1): 203 – 225

Bonnet NJ, Beauvais A, Arnaud N, Chardon D and Jayananda M. 2016. Cenozoic lateritic weathering and erosion history of Peninsular India from $^{40}Ar/^{39}$ Ar dating of supergene K-Mn oxides. Chemical Geology, 446: 33 – 53

Bouzari F and Clark AH. 2002. Anatomy, evolution, and metallogenic significance of the supergene orebody of the Cerro Colorado porphyry copper deposit, I Región, northern Chile. Economic Geology, 97(8): 1701 – 1740

Burnard PG, Hu R, Turner G and Bi XW. 1999. Mantle, crustal and atmospheric noble gases in Ailaoshan gold deposits, Yunnan Province, China. Geochimica et Cosmochimica Acta, 63(10): 1595 – 1604

Burnard PG and Polya DA. 2004. Importance of mantle derived fluids during granite associated hydrothermal circulation: He and Ar isotopes of ore minerals from Panasqueira. Geochimica et Cosmochimica Acta, 68(7): 1607 – 1615

Cai MH, Wang XB, Nagao K, Peng ZA, Guo TF, Liu H and Tan ZM. 2012. Noble gas isotopic characteristics of Hehuaping tin-polymetallic deposit, southern Hunan Province. Mineral Deposits, 31(6): 1163 – 1170 (in Chinese with English abstract)

Cai MH, Peng ZA, Nagao K, Wang XB, Guo TF and Liu H. 2013. Isotopic characteristics of noble gases of the Fuchuan-Hezhou-Zhongshan W-Sn-polymetallic ore concentration area in northeastern Guangxi and their geological significance. Acta Geoscientica Sinica, 34(3): 287 – 294 (in Chinese with English abstract)

Camprubí A, Chomiak BA, Villanueva-Estrada RE, Canals À, Norman DI, Cardellach E and Stute M. 2006. Fluid sources for the La Guitarra epithermal deposit (Temascaltepec district, Mexico): Volatile and helium isotope analyses in fluid inclusions. Chemical Geology, 231(3): 252 – 284

Chen J, Lu JJ, Chen WF, Wang RC, Ma DS, Zhu JC, Zhang WL and Ji JF. 2008. W-Sn-Nb-Ta-bearing granites in the Nanling Range and their relationship to metallogengesis. Geological Journal of China Universities, 14(4): 459 – 473 (in Chinese with English abstract)

Chen L and Li JW. 2014. $^{40}Ar/^{39}$ Ar ages and stable isotopes of supergene jarosite from the Baiyin VHMS ore field, NE Tibetan Plateau with paleoclimatic implications. Chinese Science Bulletin, 59(24): 2999 – 3009

Chen W and Zhang Y. 2010. (U-Th)/He dating laboratory was built in the China Geological Survey system. Geology in China, 37(3): 840 (in Chinese)

Chen X, Su WC and Huang Y. 2016. He and Ar isotope Geochemistry of ore-forming fluids for the Qinglong Sb deposit in Guizhou Province, China. Acta Petrologica Sinica, 32(11): 3312 – 3320 (in Chinese with English abstract)

Chen YJ, Pirajno F and Qi JP. 2008. The Shanggong gold deposit, Eastern Qinling Orogen, China: Isotope geochemistry and implications for ore genesis. Journal of Asian Earth Sciences, 33(3 – 4): 252 – 266

Chen ZB. 1985. Some basic metallogenetic aspects on Phanerozoic vein-type uranium deposits. Uranium Geology, 1(1): 1 – 15 (in Chinese with English abstract)

Chukhrov FV, Yermilova LP and Shanin LL. 1969. Age of alunite from certain deposits. Trans. Acad. Sci. USSR Dokl., Earth-Sci. Sect., 185: 49 – 51

Craig H and Lupton JE. 1976. Primordial neon, helium, and hydrogen in oceanic basalts. Earth and Planetary Science Letters, 31(3): 369 – 385

Danišík M, Evans NJ, Ramanaidou ER, McDonald BJ, Mayers C and McInnes BIA. 2013. (U-Th)/He chronology of the Robe River channel iron deposits, Hamersley Province, Western Australia. Chemical Geology, 354: 150 – 162

Davidheiser-Kroll B, Stuart FM and Boyce AJ. 2014. Mantle heat drives hydrothermal fluids responsible for carbonate-hosted base metal deposits: Evidence from $^{3}He/^{4}He$ of ore fluids in the Irish Pb-Zn ore district. Mineralium Deposita, 49(5): 547 – 553

De Putter T, Ruffet G, Yans J and Mees F. 2015. The age of supergene manganese deposits in Katanga and its implications for the Neogene evolution of the African Great Lakes Region. Ore Geology Reviews, 71: 350 – 362

Deng XD, Li JW, Vasconcelos PM, Cohen BE and Kusky TM. 2014. Geochronology of the Baye Mn oxide deposit, southern Yunnan Plateau: Implications for the late Miocene to Pleistocene paleoclimatic conditions and topographic evolution. Geochimica et Cosmochimica Acta, 139: 227 – 247

Deng XD, Li JW and Vasconcelos PM. 2016. $^{40}Ar/^{39}$ Ar dating of supergene Mn-oxides from the Zunyi Mn deposit, Guizhou Plateau, SW China: Implications for chemical weathering and paleoclimatic evolution since the late Miocene. Chemical Geology, 445: 185 – 198

Deng XD, Li JW and Shuster DL. 2017. Late Mio-Pliocene chemical weathering of the Yulong porphyry Cu deposit in the eastern Tibetan Plateau constrained by goethite (U-Th)/He dating: Implication for Asian summer monsoon. Earth and Planetary Science Letters, 472: 289 – 298

Desanois L, Lüders V, Niedermann S and Trumbull RB. 2018. Formation of epithermal Sn-Ag-(Zn) vein-type mineralization at the Pirquitas deposit, NW Argentina: Fluid inclusion and noble gas isotopic constraints. Chemical Geology, doi: 10.1016/j.chemgeo.2018.04.024

Dobson KJ, Stuart FM and Dempster TJ. 2008. U and Th zonation in Fish Canyon Tuff zircons: Implications for a zircon (U-Th)/He standard. Geochimica et Cosmochimica Acta, 72(19): 4745 – 4755

Ershova V, Anfinson O, Prokopiev A, Khudoley A, Stockli D, Faleide JI, Gaina C and Malyshev N. 2018. Detrital zircon (U-Th)/He ages from Paleozoic strata of the Severnaya Zemlya Archipelago: Deciphering multiple episodes of Paleozoic tectonic evolution within the Russian High Arctic. Journal of Geodynamics, 119: 210 – 220

Evans NJ, Byrne JP, Keegan JT and Dotter LE. 2005. Determination of uranium and thorium in zircon, apatite, and fFluorite: Application to laser (U-Th)/He thermochronology. Journal of Analytical Chemistry, 60(12): 1159 – 1165

Evenson NS, Reiners PW, Spencer JE and Shuster DL. 2014. Hematite and Mn oxide (U-Th)/He dates from the Buckskin-Rawhide detachment system, western Arizona: Gaining insights into hematite (U-Th)/He systematics. American Journal of Science, 314(10): 1373 – 1435

Fan CY, Zhu BQ, Pu ZP, Zhang QF and Dai GY. 1986. Investigation on pyrite $^{39}Ar/^{40}$ Ar dating. Third Chinese Conference on Isotope Geochemistry, 249 – 250 (in Chinese)

Fanale FP and Kulp JL. 1962. The helium method and the age of the Cornwall, Pennsylvania magnetite ore. Economic Geology, 57(5): 735 – 746

Farley KA, Kohn BP and Pillans B. 2002. The effects of secular disequilibrium on (U-Th)/He systematics and dating of Quaternary volcanic zircon and apatite. Earth and Planetary Science Letters, 201(1): 117 – 125

Farley KA and Flowers RM. 2012. (U-Th)/Ne and multidomain (U-Th)/He systematics of a hydrothermal hematite from eastern Grand Canyon. Earth and Planetary Science Letters, 359 – 360: 131 – 140

Farley KA. 2018. Helium diffusion parameters of hematite from a single-diffusion-domain crystal. Geochimica et Cosmochimica Acta, 231: 117 – 129

Flowers RM, Ketcham RA, Shuster DL and Farley KA. 2009. Apatite (U-Th)/He thermochronometry using a radiation damage accumulation and annealing model. Geochimica et Cosmochimica Acta, 73(8): 2347 – 2365

Garcia VH and Reiners PW. 2015. Secondary Fe-and Mn-oxides associated with faults near Moab, Utah: Records of past fluid flow. In: American Geophysical Union, Fall Meeting 2015. Washington: AGU

Gautheron C and Moreira M. 2002. Helium signature of the subcontinental lithospheric mantle. Earth and Planetary Science Letters, 199(1 – 2): 39 – 47

Goldfarb RJ, Hart C, Davis G and Groves D. 2007. East Asian gold: Deciphering the anomaly of Phanerozoic gold in Precambrian cratons.

Economic Geology, 102(3): 341 - 345
Graham DW. 2002. Noble gas isotope geochemistry of mid-ocean ridge and ocean island basalts: Characterization of mantle source reservoirs. Reviews in Mineralogy and Geochemistry, 47(1): 247 - 317
Graupner T, Niedermann S, Kempe U, Klemd R and Bechtel A. 2006. Origin of ore fluids in the Muruntau gold system: Constraints from noble gas, carbon isotope and halogen data. Geochimica et Cosmochimica Acta, 70(21): 5356 - 5370
Harris AC, Dunlap WJ, Reiners PW, Allen CM, Cooke DR, White NC, Campbell IH and Golding SD. 2008. Multimillion year thermal history of a porphyry copper deposit: Application of U-Pb, $^{40}Ar/^{39}Ar$ and (U-Th)/He chronometers, Bajo de la Alumbrera copper-gold deposit, Argentina. Mineralium Deposita, 43(3): 295 - 314
Hart CJR, Goldfarb RJ, Qiu YM, Snee L. Miller LD and Miller ML. 2002. Gold deposits of the northern margin of the North China Craton: Multiple late Paleozoic-Mesozoic mineralizing events. Mineralium Deposita, 37(3 - 4): 326 - 351
Hattori KH and Keith JD. 2001. Contribution of mafic melt to porphyry copper mineralization: Evidence from Mount Pinatubo, Philippines, and Bingham Canyon, Utah, USA. Mineralium Deposita, 36(8): 799 - 806
He W, Li DM, Zheng DW, Wan JL and Xu YX. 2009. K-Ar dating of Jarosite in eastern Tianshan and its environmental significances. Seismology and Geology, 31(3): 415 - 423 (in Chinese with English abstract)
Heim JA, Vasconcelos PM, Shuster DL, Farley KA and Broadbent G. 2006. Dating paleochannel iron ore by (U-Th)/He analysis of supergene goethite, Hamersley province, Australia. Geology, 34(3): 173 - 176
Horne AM, van Soest MC, Hodges KV, Tripathy-Lang A and Hourigan JK. 2016. Integrated single crystal laser ablation U/Pb and (U-Th)/He dating of detrital accessory minerals: Proof-of-concept studies of titanites and zircons from the Fish Canyon tuff. Geochimica et Cosmochimica Acta, 178: 106 - 123
Hu RG, Wang M, Wijbrans JR, Brouwer FM and Qiu HN. 2013. $^{40}Ar/^{39}Ar$ geochronology of amphibole from the amphibolite rocks, Xitieshan terrane, North Qaidam UHP metamorphic belt, western China. Acta Petrologica Sinica, 29(9): 3031 - 3038 (in Chinese with English abstract)
Hu RG, Wijbrans JR, Brouwer FM, Zhao LH, Wang M and Qiu HN. 2015. Retrograde metamorphism of the eclogite in North Qaidam, western China: Constraints by joint $^{40}Ar/^{39}Ar$ in vacuo crushing and stepped heating. Geoscience Frontiers, 6(5): 759 - 770
Hu RG, Wijbrans JR, Brouwer FM, Wang M, Zhao LH and Qiu HN. 2016. $^{40}Ar/^{39}Ar$ thermochronological constraints on the retrogression and exhumation of ultra-high pressure (UHP) metamorphic rocks from Xitieshan terrane, North Qaidam, China. Gondwana Research, 36: 157 - 175
Hu RZ, Burnard PG, Turner G and Bi XW. 1998a. Helium and argon isotope systematics in fluid inclusions of Machangqing copper deposit in west Yunnan Province, China. Chemical Geology, 146(1 - 2): 55 - 63
Hu RZ, Turner G, Burnard PG, Zhong H, Ye ZJ and Bi XW. 1998b. Helium and argon isotopic geochemistry of Jinding superlarge Pb-Zn deposit. Science in China (Series D), 41(4): 442 - 448
Hu RZ, Turner G, Burnard PG and Bi XW. 1998c. Helium isotope compositions of Machangqing copper deposit in western Yunnan, China. Chinese Science Bulletin, 43(1): 69 - 72
Hu RZ, Bi XW, Turner G and Burnard PG. 1999. Helium and argon isotope geochemistry of the ore-forming fluid for gold deposits in Ailaoshan metallogenic belt. Science in China (Series D), 29(4): 321 - 330 (in Chinese)
Hu RZ, Burnard PG, Bi XW, Zhou MF, Peng JT, Su WC and Wu KX. 2004. Helium and argon isotope geochemistry of alkaline intrusion-associated gold and copper deposits along the Red River-Jinshajiang fault belt, SW China. Chemical Geology, 203(3 - 4): 305 - 317
Hu RZ, Bi XW, Zhou MF, Peng JT, Su WC, Liu S and Qi HW. 2008. Uranium metallogenesis in South China and its relationship to crustal extension during the Cretaceous to Tertiary. Economic Geology, 103(3): 583 - 598
Hu RZ, Burnard PG, Bi XW, Zhou MF, Peng JT, Su WC and Zhao JH. 2009. Mantle-derived gaseous components in ore-forming fluids of the Xiangshan uranium deposit, Jiangxi Province, China: Evidence from He, Ar and C isotopes. Chemical Geology, 266(1 - 2): 86 - 95
Hu RZ, Bi XW, Jiang GH, Chen HW, Peng JT, Qi YQ, Wu LY and Wei WF. 2012. Mantle-derived noble gases in ore-forming fluids of the granite-related Yaogangxian tungsten deposit, southeastern China. Mineralium Deposita, 47(6): 623 - 632
Hua RM, Chen PR, Zhang WL, Liu XD, Lu JJ, Lin JF, Yao JM, Qi HW, Zhang ZS and Gu SY. 2003. Metallogenic systems related to Mesozoic and Cenozoic granitoids in South China. Science in China (Series D), 46(8): 816 - 829
Hurley PM and Goodman C. 1943. Helium age measurement. Ⅰ. Preliminary magnetite index. GSA Bulletin, 54(3): 305 - 324
Irwin JJ and Roedder E. 1995. Diverse origins of fluid in magmatic inclusions at Bingham (Utah, USA), Butte (Montana, USA), St. Austell (Cornwall, UK), and Ascension Island (mid-Atlantic, UK), indicated by laser microprobe analysis of Cl, K, Br, I, Ba + Te, U, Ar, Kr, and Xe. Geochimica et Cosmochimica Acta, 59(2): 295 - 312
Jean-Baptiste P and FouquET Y. 1996. Abundance and isotopic composition of helium in hydrothermal sulfides from the East Pacific Rise at 13°N. Geochimica et Cosmochimica Acta, 60(1): 87 - 93
Jean-Baptiste P, Bougault H, Vangriesheim A, Charlou JL, Radford-Knoery J, Fouquet Y, Needham D and German C. 1998. Mantle ^{3}He in hydrothermal vents and plume of the Lucky Strike site (MAR 37°17′) and associated geothermal heat flux. Earth and Planetary Science Letters, 157(1 - 2): 69 - 77
Jiang SY, Dai BZ, Jiang YH, Zhao HX and Hou ML. 2009. Jiaodong and Xiaoqinling: Two orogenic gold provinces formed in different tectonic settings. Acta Petrologica Sinica, 25(11): 2727 - 2738 (in Chinese with English abstract)
Jiang YD, Qiu HN, Yun JB and Wang Q. 2007. Sphalerite $^{40}Ar/^{39}Ar$ dating by crushing in vacuum and stepwise heating on crushed powders. Geochimica, 36(5): 457 - 466 (in Chinese with English abstract)
Jiang YD, Qiu HN and Xu YG. 2012. Hydrothermal fluids, argon isotopes and mineralization ages of the Fankou Pb-Zn deposit in South China: Insights from sphalerite $^{40}Ar/^{39}Ar$ progressive crushing. Geochimica et Cosmochimica Acta, 84: 369 - 379
Kelley S, Turner G, Butterfield AW and Shepherd TJ. 1986. The source and significance of argon isotopes in fluid inclusions from areas of mineralization. Earth and Planetary Science Letters, 79(3 - 4): 303 - 318
Kendrick MA, Burgess R, Pattrick RAD and Turner G. 2001a. Fluid inclusion noble gas and halogen evidence on the origin of Cu-porphyry mineralising fluids. Geochimica et Cosmochimica Acta, 65(16): 2651 - 2668
Kendrick MA, Burgess R, Pattrick RAD and Turner G. 2001b. Halogen and Ar-Ar age determinations of inclusions within quartz veins from porphyry copper deposits using complementary noble gas extraction techniques. Chemical Geology, 177(3 - 4): 351 - 370
Kendrick MA, Burgess R, Pattrick RA and Turner G. 2002. Hydrothermal fluid origins in a fluorite-rich Mississippi valley-type district: Combined noble gas (He, Ar, Kr) and halogen (Cl, Br, I) analysis of fluid inclusions from the South Pennine ore field, United Kingdom. Economic Geology, 97(3): 435 - 451
Kendrick MA, Burgess R, Harrison D and Bjørlykke A. 2005. Noble gas and halogen evidence for the origin of Scandinavian sandstone-hosted Pb-Zn deposits. Geochimica et Cosmochimica Acta, 69(1): 109 - 129
Kendrick MA, Mark G and Phillips D. 2007. Mid-crustal fluid mixing in a Proterozoic Fe oxide-Cu-Au deposit, Ernest Henry, Australia: Evidence from Ar, Kr, Xe, Cl, Br, and I. Earth and Planetary

Science Letters, 256(3-4): 328-343
Kendrick MA, Honda M, Walshe J and Petersen K. 2011a. Fluid sources and the role of abiogenic-CH_4 in Archean gold mineralization: Constraints from noble gases and halogens. Precambrian Research, 189(3-4): 313-327
Kendrick MA, Phillips D, Wallace M and Miller JM. 2011b. Halogens and noble gases in sedimentary formation waters and Zn-Pb deposits: A case study from the Lennard Shelf, Australia. Applied Geochemistry, 26(12): 2089-2100
Kendrick MA and Burnard P. 2013. Noble gases and halogens in fluid inclusions: A journey through the Earth's crust. In: Burnard P (ed.). The Noble Gases as Geochemical Tracers. Berlin, Heidelberg: Springer, 319-369
Kula J and Baldwin SL. 2012. On hematite as a target for dating aqueous conditions on Mars. Planetary and Space Science, 67(1): 101-108
Kurz MD. 1986. Cosmogenic helium in a terrestrial igneous rock. Nature, 320(6061): 435-439
Li GM, Cao MJ, Qin KZ, Evans NJ, McInnes BIA and Liu YS. 2014. Thermal-tectonic history of the Baogutu porphyry Cu deposit, West Junggar as constrained from zircon U-Pb, biotite Ar/Ar and zircon/apatite (U-Th)/He dating. Journal of Asian Earth Sciences, 79: 741-758
Li JW, Vasconcelos PM and Zhang J. 2002. Behavior of argon gas release from manganese oxide minerals as revealed by $^{40}Ar/^{39}Ar$ laser incremental heating analysis. Chinese Science Bulletin, 47(18): 1502-1510
Li JW, Yan DR, Vasconcelos PM, Duzgoren-Aydin NS, Hu MA and Chen MH. 2004. $^{40}Ar/^{39}Ar$ geochronology of supergene K-bearing manganese oxides and its paleoclimatic implications. Earth Science Frontiers, 11(2): 589-598 (in Chinese with English abstract)
Li JW, Bi SJ, Selby D, Chen L, Vasconcelos P, Thiede D, Zhou MF, Zhao XF, Li ZK and Qiu HN. 2012. Giant Mesozoic gold provinces related to the destruction of the North China craton. Earth and Planetary Science Letters, 349-350: 26-37
Li XH, Chu FY, Lei JJ, Zhao HQ and Yu X. 2014. Discussion on sources of metallogenic materials of hydrothermal sulfide from Southwest Indian Ridge: Isotope evidences. Journal of Earth Sciences and Environment, 36(1): 193-200 (in Chinese with English abstract)
Li ZL, Hu RZ, Peng JT, Bi XW and Li XM. 2006. Helium isotope geochemistry of ore-forming fluids from Furong tin orefield in Hunan Province, China. Resource Geology, 56(1): 9-15
Li ZL, Hu RZ, Yang JS, Peng JT, Li XM and Bi XW. 2007. He, Pb and S isotopic constraints on the relationship between the A-type Qitianling granite and the Furong tin deposit, Hunan Province, China. Lithos, 97(1-2): 161-173
Lippolt HJ, Wernicke RS and Boschmann W. 1993. ^4He diffusion in specular hematite. Physics and Chemistry of Minerals, 20(6): 415-418
Lippolt HJ, Wernicke RS and Baähr R. 1995. Paragenetic specularite and adularia (Elba, Italy): Concordant (U+Th)-He and K-Ar ages. Earth and Planetary Science Letters, 132(1-4): 43-51
Lippolt HJ, Brander T and Mankopf NR. 1998. An attempt to determine formation ages of goethites and limonites by $(U+Th)-^4He$ dating. Neues Jahrbuch fur Mineralogie Monatshefte, 11: 505-528
Liu J, Wu G, Qiu HN, Gao DZ and Yang XS. 2013. $^{40}Ar/^{39}Ar$ dating of gold-bearing quartz vein from the Shabaosi gold deposit at the northern end of the Great Xing'an Range and its tectonic significance. Acta Geologica Sinica, 87(10): 1570-1579 (in Chinese with English abstract)
Lu HZ. 1986. Origin of Tungsten Mineral Deposit in South China. Chongqing: Publishing House of Chongqing, 1-232 (in Chinese with English abstract)
Lupton JE, Klinkhammer GP, Normark WR, Haymon R, MacDonald KC, Weiss RF and Craig H. 1980. Helium-3 and manganese at the 21°N East Pacific Rise hydrothermal site. Earth and Planetary Science Letters, 50(1): 115-127
Lupton JE, Baker ET and Massoth GJ. 1989. Variable ^3He/heat ratios in submarine hydrothermal systems: Evidence from two plumes over the Juan de Fuca ridge. Nature, 337(6203): 161-164
Lupton JE, Baker ET, Massoth GJ, Thomson RE, Burd BJ, Butterfield DA, Embley RW and Cannon GA. 1995. Variations in water-column ^3He/heat ratios associated with the 1993 CoAxial event, Juan de Fuca Ridge. Geophysical Research Letters, 22(2): 155-158
Manning AH and Hofstra AH. 2017. Noble gas data from Goldfield and Tonopah epithermal Au-Ag deposits, ancestral Cascades Arc, USA: Evidence for a primitive mantle volatile source. Ore Geology Reviews, 89: 683-700
Mao JW, Goldfarb RJ, Zhang ZW, Xu WY, Qiu YM and Deng J. 2002. Gold deposits in the Xiaoqinling-Xiong'ershan region, Qinling Mountains, central China. Mineralium Deposita, 37(3-4): 306-325
Mao JW, Li YQ, Goldfarb R, He Y and Zaw K. 2003. Fluid Inclusion and noble gas studies of the Dongping gold deposit, Hebei Province, China: A mantle connection for mineralization? Economic Geology, 98(3): 517-534
McDermott R, Ault AK, Evans JP, Reiners PW and Shuster DL. 2015. Integrating hematite (U-Th)/He dating, microtextural analysis, and thermomechanical modeling to date seismic slip. In: American Geophysical Union, Fall Meeting 2015. Washington: AGU
Merrihue C and Turner G. 1966. Potassium-argon dating by activation with fast neutrons. Journal of Geophysical Research Atmospheres, 71(11): 2852-2857
Monteiro HS, Vasconcelos PM, Farley KA, Spier CA and Mello CL. 2014. (U-Th)/He geochronology of goethite and the origin and evolution of cangas. Geochimica et Cosmochimica Acta, 131: 267-289
Morelli R, Creaser RA, Seltmann R, Stuart FM, Selby D and Graupner T. 2007. Age and source constraints for the giant Muruntau gold deposit, Uzbekistan, from coupled Re-Os-He isotopes in arsenopyrite. Geology, 35(9): 795-798
Mote TI, Becker TA, Renne P and Brimhall GH. 2001. Chronology of exotic mineralization at El Salvador, Chile, by $^{40}Ar/^{39}Ar$ dating of copper wad and supergene alunite. Economic Geology, 96(2): 351-366
O'Nions RK and Oxburgh ER. 1983. Heat and helium in the earth. Nature, 306(5942): 429-431
Pettke T, Frei R, Kramers JD and Villa IM. 1997. Isotope systematics in vein gold from Brusson, Val d'Ayas (NW Italy) 3. (U+Th)/He and K/Ar in native Au and its fluid inclusions. Chemical Geology, 135(3-4): 173-187
Phillips D and Miller JM. 2006. $^{40}Ar/^{39}Ar$ dating of mica-bearing pyrite from thermally overprinted Archean gold deposits. Geology, 34(5): 397-400
Podosek FA, Bernatowicz TJ and Kramer FE. 1981. Adsorption of xenon and krypton on shales. Geochimica et Cosmochimica Acta, 45(12): 2401-2415
Qiu HN and Dai TM. 1989. $^{40}Ar/^{39}Ar$ technique for dating the fluid inclusions of quartz from a hydrothermal deposit. Chinese Science Bulletine, 34(22): 1887-1890
Qiu HN, Dai TM and Pu ZP. 1994. Dating mineralization of Lushui tin-tungsten deposit, Western Yunnan, using $^{40}Ar-^{39}Ar$ age spectrum technique. Geochimica, 23(Suppl.): 93-102 (in Chinese with English abstract)
Qiu HN. 1996. $^{40}Ar-^{39}Ar$ dating of the quartz sample from two mineral deposits in western Yunnan (SW China) by crushing in vacuum. Chemical Geology, 127(1-3): 211-222
Qiu HN, Sun DZ, Zhu BQ and Chang XY. 1997. Isotope geochemistry study of Dongchuan copper deposits in middle Yunnan province, SW China: Ⅱ. Dating the ages of mineralizations by Pb-Pb and $^{40}Ar-^{39}Ar$ methods. Geochimica, 26(2): 39-45 (in Chinese with English abstract)
Qiu HN, Zhu BQ and Sun DZ. 2000. $^{40}Ar-^{39}Ar$ dating techniques for a hydrothermal siliceous breccia sample from the Luoxue mine,

Dongchuan copper deposits, Yuunan, by crushing in vacuum and then by stepped heating on its powders. Geochimica, 29(1): 21 - 27 (in Chinese with English abstract)

Qiu HN, Wijbrans JR, Li XH, Zhu BQ, Zhu CL and Zeng BC. 2001. ^{40}Ar-^{39}Ar dating for the mineralization ages of the Dongchuan-type layered copper deposits, Yunnan. Bulletin of Mineralogy, Petrology and Geochemistry, 20(4): 358 - 359 (in Chinese with English abstract)

Qiu HN, Zhu BQ and Sun DZ. 2002. Age significance interpreted from ^{40}Ar-^{39}Ar dating of quartz samples from the Dongchuan copper deposits, Yunnan, SW China, by crushing and heating. Geochemical Journal, 36(5): 475 - 491

Qiu HN, Wijbrans JR, Li XH, Zhu BQ, Zhu CL and Zeng BC. 2002. New ^{40}Ar-^{39}Ar evidence for ore-forming process during Jinning-Chengjiang Period in Dongchuan type copper deposits, Yunnan. Mineral Deposits, 21(2): 129 - 136 (in Chinese with English abstract)

Qiu HN, Wijbrans JR, Shi HS and Li FL. 2004. The 450Ma message and excess ^{40}Ar within garnet from the Bixiling eclogite in Dabie Shan: Interpreted from the ^{40}Ar-^{39}Ar dating results by crushing. Geochimica, 33(4): 325 - 333 (in Chinese with English abstract)

Qiu HN and Wijbrans JR. 2006. Paleozoic ages and excess ^{40}Ar in garnets from the Bixiling eclogite in Dabieshan, China: New insights from $^{40}Ar/^{39}Ar$ dating by stepwise crushing. Geochimica et Cosmochimica Acta, 70(9): 2354 - 2370

Qiu HN and Wijbrans JR. 2006. Amphibolite-facies overprinting and a hydrothermal activity in southern Dabie terrane: Insight from Ar-Ar dating of Zhujiachong eclogite and metamorphic amphibole vein. Geochimica, 35(5): 517 - 524 (in Chinese with English abstract)

Qiu HN and Jiang YD. 2007. Sphalerite $^{40}Ar/^{39}Ar$ progressive crushing and stepwise heating techniques. Earth and Planetary Science Letters, 256(1 - 2): 224 - 232

Qiu HN and Wijbrans JR. 2008. The Paleozoic metamorphic history of the Central Orogenic Belt of China from $^{40}Ar/^{39}Ar$ geochronology of eclogite garnet fluid inclusions. Earth and Planetary Science Letters, 268(3 - 4): 501 - 514

Qiu HN, Xu YG, Yun JB, Wang Q and Zhao LH. 2009. ^{40}Ar-^{39}Ar Ultra-Violet Laser Ablation Microprobe (UVLAMP): Timing of amphibolite-facies retrograde metamorphism of Zhujiachong UHP eclogite. Acta Geologica Sinica, 83(8): 1118 - 1124 (in Chinese with English abstract)

Qiu HN, Wijbrans JR, Brouwer FM, Yun JB, Zhao LH and Xu YG. 2010a. Amphibolite facies retrograde metamorphism of the Zhujiachong eclogite, SE Dabieshan: $^{40}Ar/^{39}Ar$ age constraints from argon extraction using UV-laser microprobe, in vacuo crushing and stepwise heating. Journal of Metamorphic Geology, 28(5): 477 - 487

Qiu NS, Wang JY, Mei QH, Jiang G and Tao C. 2010b. Constraints of (U-Th)/He ages on Early Paleozoic tectonothermal evolution of the Tarim Basin, China. Science China (Earth Sciences), 53(7): 964 - 976

Quang CX, Clark AH, Lee JKW and Guillen BJ. 2003. ^{40}Ar-^{39}Ar ages of hypogene and supergene mineralization in the Cerro Verde-Santa Rosa porphyry Cu-Mo cluster, Arequipa, Peru. Economic Geology, 98(8): 1683 - 1696

Quang CX, Clark AH, Lee JKW and Hawkes N. 2005. Response of supergene processes to episodic Cenozoic uplift, pediment erosion, and ignimbrite eruption in the porphyry copper province of southern Perú. Economic Geology, 100(1): 87 - 114

Reiners PW and Farley KA. 1999. Helium diffusion and (U-Th)/He thermochronometry of titanite. Geochimica et Cosmochimica Acta, 63(22): 3845 - 3859

Reiners PW, Farley KA and Hickes HJ. 2002. He diffusion and (U-Th)/He thermochronometry of zircon: Initial results from Fish Canyon Tuff and Gold Butte. Tectonophysics, 349(1 - 4): 297 - 308

Reiners PW, Zhou ZY, Ehlers TA, Xu CH, Brandon MT, Donelick RA and Nicolescu S. 2003. Post-orogenic evolution of the Dabie Shan, eastern China, from (U-Th)/He and fission-track thermochronology. American Journal of Science, 303(6): 489 - 518

Reiners PW, Shuster DL and Evenson N. 2015. Formation ages and thermal histories of fracture-filling hematite and Mn-oxide in Precambrian basement from (U-Th)/He dating and $^{4}He/^{3}He$ diffusion experiments. In: American Geophysical Union, Fall Meeting 2015. Washington: AGU

Richard A, Kendrick MA and Cathelineau M. 2014. Noble gases (Ar, Kr, Xe) and halogens (Cl, Br, I) in fluid inclusions from the Athabasca Basin (Canada): Implications for unconformity-related U deposits. Precambrian Research, 247: 110 - 125

Riffel SB, Vasconcelos PM, Carmo IO and Farley KA. 2015. Combined $^{40}Ar/^{39}Ar$ and (U-Th)/He geochronological constraints on long-term landscape evolution of the Second Paraná Plateau and its ruiniform surface features, Paraná, Brazil. Geomorphology, 233: 52 - 63

Ruffet G, Innocent C, Michard A, Féraud G, Beauvais A, Nahon D and Hamelin B. 1996. A geochronological $^{40}Ar/^{39}Ar$ and $^{87}Rb/^{87}Sr$ study of K-Mn oxides from the weathering sequence of Azul, Brazil. Geochimica et Cosmochimica Acta, 60(12): 2219 - 2232

Sánchez V, Stuart FM, Martín-Crespo T, Vindel E, Corbella M and Cardellach E. 2010. Helium isotopic ratios in fluid inclusions from fluorite-rich Mississippi Valley-Type district of Asturias, northern Spain. Geochemical Journal, 44(6): E1-E4

Shan Q, Zeng QS, Li JK, Lu HZ, Hou MZ, Yu XY and Wu CJ. 2014. Diagenetic and metallogenic sources of Furong Tin deposit, Qitianling: Constraints from Lu-Hf for zircon and He-Ar isotope for fluid inclusions. Acta Geologica Sinica, 88(4): 704 - 715 (in Chinese with English abstract)

Shukolyukov YA, Yakubovich OV and Rytsk YA. 2010. About possibility of isotope dating of native gold by the (U-Th)/He method. Doklady Earth Sciences, 430(1): 90 - 94

Shuster DL, Vasconcelos PM, Heim JA and Farley KA. 2005. Weathering geochronology by (U-Th)/He dating of goethite. Geochimica et Cosmochimica Acta, 69(3): 659 - 673

Sillitoe RH and McKee EH. 1996. Age of supergene oxidation and enrichment in the Chilean porphyry copper province. Economic Geology, 91(1): 164 - 179

Simmons SF, Sawkins FJ and Schlutter DJ. 1987. Mantle-derived helium in two Peruvian hydrothermal ore deposits. Nature, 329(6138): 429 - 432

Smith PE, Evensen NM, York D, Szatmari P and de Oliveira DC. 2001. Single-crystal ^{40}Ar-^{39}Ar dating of pyrite: No fool's clock. Geology, 29(5): 403 - 406

Smith PE, Evensen NM, York D and Moorbath S. 2005. Oldest reliable terrestrial ^{40}Ar-^{39}Ar age from pyrite crystals at Isua West Greenland. Geophysical Research Letters, 32(21): L21318

Stockli DF and Farley KA. 2004. Empirical constraints on the titanite (U-Th)/He partial retention zone from the KTB drill hole. Chemical Geology, 207(3 - 4): 223 - 236

Strutt RJ. 1908. On the accumulation of helium in geological time. Proceedings of the Royal Society of London. Series A, Containing Papers of a Mathematical and Physical Character, 81(547): 272 - 277

Strutt RJ. 1910. The accumulation of helium in geological time. Ⅲ. Proceedings of the Royal Society of London. Series A, Containing Papers of a Mathematical and Physical Character, 83(562): 289 - 301

Stuart FM and Turner G. 1992. The abundance and isotopic composition of the noble gases in ancient fluids. Chemical Geology (Isotope Geoscience Section), 101(1 - 2): 97 - 109

Stuart FM, Turner G and Taylor R. 1994a. He-Ar isotope systematics of fluid inclusions: Resolving mantle and crustal contributions to hydrothermal fluids. In: Matsuda J (ed.). Noble Gas Geochemistry and Cosmochemistry. Tokyo: Terra Scientific Publishing Company, 261 - 277

Stuart FM, Turner G, Duckworth RC and Fallick AE. 1994b. Helium isotopes as tracers of trapped hydrothermal fluids in ocean-floor

sulfides. Geology, 22(9): 823 – 826

Stuart FM, Burnard PG, Taylor RP and Turner G. 1995. Resolving mantle and crustal contributions to ancient hydrothermal fluids: He–Ar isotopes in fluid inclusions from Dae Hwa W–Mo mineralisation, South Korea. Geochimica et Cosmochimica Acta, 59(22): 4663 – 4673

Sun JB, Chen W, Yu S, Shen Z and Tian YT. 2017. Study on zircon (U–Th) / He dating technique. Acta Petrologica Sinica, 33(6): 1947 – 1956 (in Chinese with English Abstract)

Tan J, Wei JH, He HY, Su F, Li YJ, Fu LB, Zhao SQ, Xiao GL, Zhang F, Xu JF, Liu Y, Stuart FM and Zhu RX. 2018. Noble gases in pyrites from the Guocheng–Liaoshang gold belt in the Jiaodong province: Evidence for a mantle source of gold. Chemical Geology, 480: 105 – 115

Tang YY, Bi XW, Fayek M, Stuart FM, Wu LY, Jiang GH, Xu LL and Liang F. 2017. Genesis of the Jinding Zn–Pb deposit, Northwest Yunnan province, China: Constraints from rare earth elements and noble gas isotopes. Ore Geology Reviews, 90: 970 – 986

Trull TW, Kurz MD and Jenkins WJ. 1991. Diffusion of cosmogenic ^{3}He in olivine and quartz: Implications for surface exposure dating. Earth and Planetary Science Letters, 103(1 – 4): 241 – 256

Turner G and Stuart FM. 1992. Helium/heat ratios and deposition temperatures of sulphides from the ocean floor. Nature, 357(6379): 581 – 583

Turner G and Wang SS. 1992. Excess argon, crustal fluids and apparent isochrons from crushing K–Feldspar. Earth and Planetary Science Letters, 110(1 – 4): 193 – 211

Turner G, Burnard P, Ford JL, Gilmour JD, Lyon IC and Stuart FM. 1993. Tracing fluid sources and interactions. Philosophical Transactions: Physical Sciences and Engineering, 344(1670): 127 – 140

Vasconcelos PM, Becker TA, Renne PR and Brimhall GH. 1992. Age and duration of weathering by ^{40}K–^{40}Ar and ^{40}Ar/^{39}Ar analysis of potassium–manganese oxides. Science, 258(5081): 451 – 455

Vasconcelos PM, Brimhall GH, Becker TA and Renne PR. 1994a. ^{40}Ar/^{39}Ar analysis of supergene jarosite and alunite: Implications to the paleoweathering history of the western USA and West Africa. Geochimica et Cosmochimica Acta, 58(1): 401 – 420

Vasconcelos PM, Renne PR, Brimhall GH and Becker TA. 1994b. Direct dating of weathering phenomena by ^{40}Ar/^{39}Ar and K–Ar analysis of supergene K–Mn oxides. Geochimica et Cosmochimica Acta, 58(6): 1635 – 1665

Vasconcelos PM. 1999. K–Ar and ^{40}Ar/^{39}Ar Geochronology of weathering processes. Annual Review of Earth and Planetary Sciences, 27: 183 – 229

Vasconcelos PM and Conroy M. 2003. Geochronology of weathering and landscape evolution, Dugald River valley, NW Queensland, Australia. Geochimica et Cosmochimica Acta, 67(16): 2913 – 2930

Wang BD, Niu SY, Sun AQ and Li HY. 2003. Helium, argon and lead isotopic compositions in gold deposits and the source of ore-forming materials in North Hebei Province. Geochimica, 32(2): 181 – 187 (in Chinese with English abstract)

Wang J and Ma LB. 2014. U–Th/He dating method of single mineral grain of apatite and zircon from Wuxi Institute of Petroleum Geology, SINOPEC. Petroleum Geology & Experiment, 36(3): 254 (in Chinese)

Wang M, Bai XJ, Hu RG, Cheng SB, Pu ZP and Qiu HN. 2015. Direct dating of cassiterite in Xitian tungsten-tin polymetallic deposit, South-East Hunan, by ^{40}Ar/^{39}Ar progressive crushing. Geotectonica et Metallogenia, 39(6): 1049 – 1060 (in Chinese with English abstract)

Wang M, Bai XJ, Yun JB, Zhao LH, Li YL, Wang ZY, Pu ZP and Qiu HN. 2016. ^{40}Ar/^{39}Ar dating of mineralization of Shizhuyuan polymetallic deposit. Geochimica, 45(1): 41 – 51 (in Chinese with English abstract)

Wang XD, Ni P, Jiang SY, Zhao KD and Wang TG. 2010. Origin of ore-forming fluid in the Piaotang tungsten deposit in Jiangxi Province: Evidence from Helium and argon isotopes. Chinese Science Bulletin, 55(7): 628 – 634

Wang Y, Zheng DW, Wu Y, Li YJ and Wang YZ. 2017. Measurement procedure of single-grain apatite (U–Th)/He dating and its validation by Durango apatite standard. Seismology and Geology, 39(6): 1143 – 1157 (in Chinese with English abstract)

Wasserburg GJ and Hayden RJ. 1955. Age of meteorites by the A^{40}–K^{40} method. Physical Review, 97(1): 86 – 87

Wei WF, Hu RZ, Bi XW, Jiang GH, Yan B, Yin RS and Yang JH. 2018. Mantle-derived and crustal He and Ar in the ore-forming fluids of the Xihuashan granite-associated tungsten ore deposit, South China. Ore Geology Reviews, under review

Weisberg WR, Metcalf JR and Flowers RM. 2018. Distinguishing slow cooling versus multiphase cooling and heating in zircon and apatite (U–Th)/He datasets: The case of the McClure Mountain syenite standard. Chemical Geology, 458: 90 – 99

Wernicke RS and Lippolt HJ. 1993. Botryoidal hematite from the Schwarzwald (Germany): Heterogeneous uranium distributions and their bearing on the helium dating method. Earth and Planetary Science Letters, 114(2 – 3): 287 – 300

Wernicke RS and Lippolt HJ. 1994a. ^{4}He age discordance and release behavior of a double shell botryoidal hematite from the Schwarzwald, Germany. Geochimica et Cosmochimica Acta, 58(1): 421 – 429

Wernicke RS and Lippolt HJ. 1994b. Dating of vein specularite using internal (U + Th)/^{4}He isochrons. Geophysical Research Letters, 21(5): 345 – 347

Wernicke RS and Lippolt HJ. 1997a. Evidence of Mesozoic multiple hydrothermal activity in the basement at Nonnenmattweiher (southern Schwarzwald), Germany. Mineralium Deposita, 32(2): 197 – 200

Wernicke RS and Lippolt HJ. 1997b. (U + Th)–He evidence of Jurassic continuous hydrothermal activity in the Schwarzwald basement, Germany. Chemical Geology, 138(3 – 4): 273 – 285

Wolf RA, Farley KA and Silver LT. 1996. Helium diffusion and low-temperature thermochronometry of apatite. Geochimica et Cosmochimica Acta, 60(21): 4231 – 4240

Worden RH. 1996. Controls on halogen concentrations in sedimentary formation waters. Mineralogical Magazine, 60(399): 259 – 274

Wu L, Wang F, Shan JN, Zhang WB, Shi WB and Feng HL. 2016. (U–Th)/He dating of international standard Durango apatite. Acta Petrologica Sinica, 32(6): 1891 – 1900 (in Chinese with English Abstract)

Wu LY, Hu RZ, Peng JT, Bi XW, Jiang GH, Chen HW, Wang QY and Liu YY. 2011. He and Ar isotopic compositions and genetic implications for the giant Shizhuyuan W–Sn–Bi–Mo deposit, Hunan Province, South China. International Geology Review, 53(5 – 6): 677 – 690

Wu LY, Hu RZ, Li XF, Sturt FM, Jiang GH, Qi YQ and Zhu JJ. 2018a. Mantle volatiles and heat contributions in high sulfidation epithermal deposit from the Zijinshan Cu–Au–Mo–Ag orefield, Fujian Province, China: Evidence from He and Ar isotopes. Chemical Geology, 480: 58 – 65

Wu LY, Sturt FM, Nicola LD, Heizler M, Benvenuti M and Hu RZ. 2018b. Multi-aliquot method for determining (U + Th)/He ages of hydrothermal hematite: Returning to Elba. Chemical Geology, doi.org/10.1016/j.chemgeo.2018.11.005

Xie GQ, Mao JW, Li W, Zhu QQ, Liu HB, Jia GH, Li YH, Li JJ and Zhang J. 2016. Different proportion of mantle-derived noble gases in the Cu–Fe and Fe skarn deposits: He–Ar isotopic constraint in the Edong district, eastern China. Ore Geology Reviews, 72(1): 343 – 354

Xu CH, Zhou ZY, Chang Y and Guillot F. 2010. Genesis of Daba arcuate structural belt related to adjacent basement upheavals: Constraints from Fission-track and (U–Th)/He thermochronology. Science China: Earth Sciences, 53(11): 1634 – 1646

Xu KQ, Sun N and Wang DZ. 1984. Petrogenesis of the granitoids and their metallogenetic relations in south China. In: Xu KQ and Tu GC (eds.). Geology of Granites and Their Metallogenetic Relations. Nanjing: Jiangsu Science and Technology Press, 1 – 31 (in

Chinese)
Xu YX, Qin KZ, Ding KS, Li JX, Miao Y, Fang TH, Xu XW, Li DM and Luo XQ. 2008. Geochronology evidence of Mesozoic metallogenesis and Cenozoic oxidation at Hongshan HS-epithermal Cu-Au deposit, Kalatage region, eastern Tianshan, and its tectonic and paleoclimatic significances. Acta Petrologica Sinica, 24(10): 2371 - 2383 (in Chinese with English abstract)
Yang J, Zheng DW and Wu Y. 2013. $^{40}Ar/^{39}Ar$ geochronology of supergene alunite-group minerals. Seismology and Geology, 35(1): 177 - 187 (in Chinese with English abstract)
Yang J, Zheng DW, Chen W, Wu Y, Li J and Zhang Y. 2015. The methodology for $^{40}Ar/^{39}Ar$ geochronology of supergene jarosite: From sampling to isotopic analysis. Geological Bulletin of China, 34(2 - 3): 579 - 586 (in Chinese with English abstract)
Yang J, Zheng DW, Chen W, Hough B, Qiu HN, Wang WT, Wu Y and Yang L. 2016. $^{40}Ar/^{39}Ar$ geochronology of supergene K-bearing sulfate minerals: Cenozoic continental weathering and its paleoclimatic significance in the Tu-Ha Basin, northwestern China. Palaeogeography, Palaeoclimatology, Palaeoecology, 445: 83 - 96
Yang JH, Wu FY and Wilde SA. 2003. A review of the geodynamic setting of large-scale Late Mesozoic gold mineralization in the North China Craton: An association with lithospheric thinning. Ore Geology Reviews, 23(3 - 4): 125 - 152
Ye XR, Wu MB, Tao MX and Sun ML. 2003. Laser microprobe analyses of noble gas isotopes in minerals: The technology and application. Earth Science Frontiers, 10(2): 293 - 300 (in Chinese with English abstract)
York D, Masliwec A, Kuybida P, Hanes JE, Hall CM, Kenyon WJ, Spooner ETC and Scott SD. 1982. $^{40}Ar/^{39}Ar$ dating of pyrite. Nature, 300(5887): 52 - 53
Yu S, Chen W, Zhang B, Sun JB, Li C, Yuan X, Shen Z, Yang L and Ma X. 2016. Mesozoic and Cenozoic uplift and exhumation history of the Kekesu section in the center Tianshan: Constrained from (U-Th)/He thermochronometry. Chinese Journal of Geophysics, 59(8): 2922 - 2936 (in Chinese with English abstract)
Zeitler PK, Herczeg AL, McDougall I and Honda M. 1987. U-Th-He dating of apatite: A potential thermochronometer. Geochimica et Cosmochimica Acta, 51(10): 2865 - 2868
Zeng ZG, Qin YS and Zhai SK. 2001. He, Ne and Ar isotope compositions of fluid inclusions in hydrothermal sulfides from the TAG hydrothermal field Mid-Atlantic Ridge. Science in China (Series D), 44(3): 221 - 228
Zeng ZG, Niedermann S, Chen S, Wang XY and Li ZX. 2015. Noble gases in sulfide deposits of modern deep-sea hydrothermal systems: Implications for heat fluxes and hydrothermal fluid processes. Chemical Geology, 409: 1 - 11
Zhai MG, Fan HR, Yang JH and Miao LC. 2004. Large-scale cluster of gold deposits in East Shandong: Anorogenic metallogenesis. Earth Science Frontiers, 11(1): 85 - 98 (in Chinese with English abstract)
Zhai W, Sun XM, Wu YS, Sun YY, Hua RM and Ye XR. 2012. He-Ar isotope geochemistry of the Yaoling-Meiziwo tungsten deposit, North Guangdong Province: Constraints on Yanshanian crust-mantle interaction and metallogenesis in SE China. Chinese Science Bulletin, 57(10): 1150 - 1159
Zhang LC, Shen YC, Li HM, Zeng QD and Liu TB. 2002. Helium and argon isotopic compositions of fluid inclusions and tracing to the source of ore-forming fluids for Jiaodong gold deposits. Acta Petrologica Sinica, 18(4): 559 - 565 (in Chinese with English abstract)
Zhang LC, Zhou XH and Ding SJ. 2008. Mantle-derived fluids involved in large-scale gold mineralization, Jiaodong District, China: Constraints provided by the He-Ar and H-O isotopic systems. International Geology Review, 50(5): 472 - 482
Zhang Y and Chen W. 2011. Study on the ^{4}He content measurement. Geological Review, 57(2): 300 - 304 (in Chinese with English abstract)
Zhang Y, Chen W and Hu M. 2011. Determination of ^{238}U, ^{232}Th and ^{147}Sm isotopes in apatites by Inductively Coupled Plasma-Mass Spectrometry with non-spike method. Rock and Mineral Analysis, 30(6): 727 - 731 (in Chinese with English abstract)
Zhu MT, Zhang LC, Wu G, He HY and Cui ML. 2013. Fluid inclusions and He-Ar isotopes in pyrite from the Yinjiagou deposit in the southern margin of the North China Craton: A mantle connection for poly-metallic mineralization. Chemical Geology, 351: 1 - 14
Zhu RX, Fan HR, Li JW, Meng QR, Li SR and Zeng QD. 2015. Decratonic gold deposits. Science China (Earth Sciences), 58(9): 1523 - 1537

附中文参考文献

白秀娟, 王敏, 卢克豪, 方金龙, 蒲志平, 邱华宁. 2011. 锡石$^{40}Ar/^{39}Ar$法直接定年探讨. 科学通报, 56(23): 1899 - 1904
蔡明海, 王显彬, 长尾敬介, 彭振安, 郭腾飞, 刘虎, 谭泽模. 2012. 湘南荷花坪锡多金属矿床稀有气体同位素特征及其地质意义. 矿床地质, 31(6): 1163 - 1170
蔡明海, 彭振安, 长尾敬介, 王显彬, 郭腾飞, 刘虎. 2013. 广西富贺钟钨锡多金属矿集区稀有气体同位素特征及其地质意义. 地球学报, 34(3): 287 - 294
陈骏, 陆建军, 陈卫锋, 王汝成, 马东升, 朱金初, 张文兰, 季峻峰. 2008. 南岭地区钨锡铌钽花岗岩及其成矿作用. 高校地质学报, 14(4): 459 - 473
陈文, 张彦. 2010. (U-Th)/He 同位素定年实验室在中国地质调查局系统内建成. 中国地质, 37(3): 840
陈娴, 苏文超, 黄勇. 2016. 贵州晴隆锑矿床成矿流体 He-Ar 同位素地球化学. 岩石学报, 32(11): 3312 - 3320
陈肇博. 1985. 显生宙脉型铀矿床成矿理论的几个基本问题. 铀矿地质, 1(1): 1 - 15
范才云, 朱炳泉, 浦志平, 张前峰, 戴桂英. 1986. 黄铁矿的$^{40}Ar/^{39}Ar$年代学研究. 第三届全国同位素地球化学学术讨论会论文(摘要)汇编, 249 - 250
何为, 李大明, 郑德文, 万景林, 许英霞. 2009. 东天山地区风化矿物黄钾铁矾的 K-Ar 测年及其环境意义. 地震地质, 31(3): 415 - 423
胡荣国, 王敏, Wijbrans JR, Brouwer FM. 邱华宁. 2013. 柴北缘锡铁山榴辉岩退变质成因角闪石$^{40}Ar/^{39}Ar$年代学研究. 岩石学报, 29(9): 3031 - 3038
胡瑞忠, 毕献武, Turner G, Burnard PG. 1999. 哀牢山金矿带金成矿流体 He 和 Ar 同位素地球化学. 中国科学(D 辑), 29(4): 321 - 330
蒋少勇, 戴宝章, 姜耀辉, 赵海香, 侯明兰. 2009. 胶东和小秦岭: 两类不同构造环境中的造山型金矿省. 岩石学报, 25(11): 2727 - 2738
蒋映德, 邱华宁, 云建兵, 王强. 2007. 闪锌矿$^{40}Ar/^{39}Ar$真空击碎与阶段加热定年技术. 地球化学, 36(5): 457 - 466
李建威, 颜代蓉, Vasconcelos PM, Duzgoren-Aydin NS, 胡明安, 陈木宏. 2004. 表生钾锰矿物$^{40}Ar/^{39}Ar$年代学及其古气候意义. 地学前缘, 11(2): 589 - 598
李小虎, 初凤友, 雷吉江, 赵宏樵, 余星. 2014. 西南印度洋中脊热液硫化物成矿物质来源探讨: 同位素证据. 地球科学与环境学报, 36(1): 193 - 200
刘军, 武广, 邱华宁, 高德柱, 杨鑫生. 2013. 大兴安岭北部砂宝斯

金矿床含金石英脉$^{40}Ar/^{39}Ar$年龄及其构造意义. 地质学报, 87(10): 1570 - 1579

卢焕章. 1986. 华南钨矿成因. 重庆: 重庆出版社, 1 - 232

邱华宁, 戴橦谟, 蒲志平. 1994. 滇西泸水钨锡矿床^{40}Ar-^{39}Ar法成矿年龄研究. 地球化学, 23(增刊): 93 - 102

邱华宁, 孙大中, 朱炳泉, 常向阳. 1997. 东川铜矿床同位素地球化学研究: II. Pb-Pb、^{40}Ar-^{39}Ar法成矿年龄测定. 地球化学, 26(2): 39 - 45

邱华宁, 朱炳泉, 孙大中. 2000. 东川铜矿硅质角砾^{40}Ar-^{39}Ar定年探. 地球化学, 29(1): 21 - 27

邱华宁, Wijbrans JR, 李献华, 朱炳泉, 朱崇林, 曾保成. 2001. "东川式"层状铜矿^{40}Ar-^{39}Ar成矿年龄测定. 矿物岩石地球化学通报, 20(4): 358 - 359

邱华宁, Wijbrans JR, 李献华, 朱炳泉, 朱崇林, 曾保成. 2002. 东川式层状铜矿^{40}Ar-^{39}Ar成矿年龄研究: 华南地区晋宁-澄江期成矿作用新证据. 矿床地质, 21(2): 129 - 136

邱华宁, Wijbrans JR, 施和生, 李发嶙. 2004. 大别山碧溪岭榴辉岩450Ma年龄信息: 石榴子石流体包裹体^{40}Ar-^{39}Ar定年初步结果. 地球化学, 33(4): 325 - 333

邱华宁, Wijbrans JR. 2006. 南大别角闪岩相退变质与热液活动: 朱家冲榴辉岩与闪石脉 Ar-Ar 年代学研究. 地球化学, 35(5): 517 - 524

邱华宁, 徐义刚, 云建兵, 王强, 赵令浩. 2009. 激光显微探针^{40}Ar-^{39}Ar定年技术——大别山朱家冲榴闪岩年代学研究. 地质学报, 83(8): 1118 - 1124

单强, 曾乔松, 李建康, 卢焕章, 侯茂洲, 于学元, 吴传军. 2014. 骑田岭芙蓉锡矿的成岩和成矿物质来源: 锆石 Lu-Hf 同位素和矿物包裹体 He-Ar 同位素证据. 地质学报, 88(4): 704 - 715

孙敬博, 陈文, 喻顺, 沈泽, 田云涛. 2017. 锆石(U-Th)/He 定年技术研究. 岩石学报, 33(6): 1947 - 1956

王宝德, 牛树银, 孙爱群, 李红阳. 2003. 冀北地区金矿床 He、Ar、Pb 同位素组成及其成矿物质来源. 地球化学, 32(2): 181 - 187

王杰, 马亮帮. 2014. 中国石化无锡石油地质研究所实验地质技术之单矿物颗粒磷灰石、锆石 U-Th/He 定年分析技术. 石油实验地质, 36(3): 254

王敏, 白秀娟, 胡荣国, 程顺波, 蒲志平, 邱华宁. 2015. 湘东南锡田钨锡多金属矿床锡石$^{40}Ar/^{39}Ar$直接定年. 大地构造与成矿学, 39(6): 1049 - 1060

王敏, 白秀娟, 云建兵, 赵令浩, 李岩林, 王周元, 蒲志平, 邱华宁. 2016. 柿竹园多金属矿床成矿作用$^{40}Ar/^{39}Ar$年代学研究. 地球化学, 45(1): 41 - 51

王英, 郑德文, 武颖, 李又娟, 王一舟. 2017. 磷灰石单颗粒(U-Th)/He 测年实验流程的建立及验证. 地震地质, 39(6): 1143 - 1157

吴林, 王非, 单竞男, 张炜斌, 师文贝, 冯慧乐. 2016. 国际标样 Durango 磷灰石(U-Th)/He 年龄测定. 岩石学报, 32(6): 1891 - 1900

徐克勤, 孙鼐, 王德滋. 1984. 华南花岗岩成因与成矿. 见: 徐克勤, 涂光炽编. 花岗岩地质和成矿关系国际学术会议论文集. 南京: 江苏科学技术出版社, 1984. 1 - 31

许英霞, 秦克章, 丁奎首, 李金祥, 缪宇, 方同辉, 徐兴旺, 李大明, 罗修泉. 2008. 东天山红山高硫型浅成低温铜-金矿床: 中生代成矿与新生代氧化的 K-Ar、Ar-Ar 年代学证据及其古构造和古气候意义. 岩石学报, 24(10): 2371 - 2383

杨静, 郑德文, 武颖. 2013. 表生明矾石族矿物$^{40}Ar/^{39}Ar$年代学概述. 地震地质, 35(1): 177 - 187

杨静, 郑德文, 陈文, 武颖, 李洁, 张彦. 2015. 风化矿物黄钾铁矾$^{40}Ar/^{39}Ar$测年的基本方法——从样品采集到年龄测试. 地质通报, 34(2 - 3): 579 - 586

叶先仁, 吴茂炳, 陶明信, 孙明良. 2003. 稀有气体同位素的激光探针分析: 技术与应用. 地学前缘, 10(2): 293 - 300

喻顺, 陈文, 张斌, 孙敬博, 李超, 袁霞, 沈泽, 杨莉, 马勋. 2016. 中天山科克苏河地区隆升剥蚀历史——来自(U-Th)/He 年龄的制约. 地球物理学报, 59(8): 2922 - 2936

翟明国, 范宏瑞, 杨进辉, 苗来成. 2004. 非造山带型金矿-胶东型金矿的陆内成矿作用. 地学前缘, 11(1): 85 - 98

张连昌, 沈远超, 李厚民, 曾庆栋, 李光明, 刘铁兵. 2002. 胶东地区金矿床流体包裹体的 He、Ar 同位素组成及成矿流体来源示踪. 岩石学报, 18(4): 559 - 565

张彦, 陈文. 2011. ^4He 同位素含量测试技术研究. 地质论评, 57(2): 300 - 304

张彦, 陈文, 胡明. 2011. 非稀释剂法电感耦合等离子体质谱测定磷灰石中铀钍钐同位素的含量. 岩矿测试, 30(6): 727 - 731